bioRxiv preprint doi: https://doi.org/10.1101/022483; this version posted July 20, 2015. The copyright holder for this preprint (which was not certified by peer review) is the author/funder, who has granted bioRxiv a license to display the preprint in perpetuity. It is made available under aCC-BY-NC-ND 4.0 International license.

Unearthing the microbial ecology of soil carbon cycling with DNA-SIP

Charles Pepe-Ranney and Ashley N Campbell * †, **Chantal Koechli** †, **Sean Berthrong, and Daniel H Buckley** † ‡

*These authors contributed equally to the manuscript and should be considered co-first authors, †School of Integrative Plant Sciences, Cornell University, New York, USA, and ‡corresponding author

Abstract

We explored the dynamics of microbial contributions to decomposition in soil by coupling DNA Stable Isotope Probing (SIP) and high throughput DNA sequencing. Our experiment evaluated the degradative succession hypothesis, described dynamics of carbon (C) metabolism during organic matter degradation, and characterized bacteria that metabolize labile and structural C in soils. We added a complex amendment representing plant derived organic matter to soil substituting ^{13}C-xylose or ^{13}C-cellulose for unlabeled equivalents in two experimental treatments which were monitored for 30 days. Xylose and cellulose are abundant components in plant biomass and represent labile and structural C pools, respectively. We characterized 5,940 SSU rRNA gene operational taxonomic units (OTUs) finding evidence for ^{13}C-incorporation into DNA from ^{13}C-xylose and ^{13}C-cellulose in 49 and 63 OTUs, respectively. In the ^{13}C-xylose treatment the types of microorganisms that incorporated ^{13}C into DNA changed over time dominated by *Firmicutes* at day 1 followed by *Bacteroidetes* at day 3 and then *Actinobacteria* at day 7. These dynamics of ^{13}C-labeling suggest labile C traveled through different trophic levels within the soil bacterial community. The microorganisms that metabolized cellulose-C increased in relative abundance over the course of the experiment with the highest number of OTUs exhibiting evidence for ^{13}C-assimilation after 14 days. Microbes that metabolized cellulose-C belonged to cosmopolitan soil lineages that remain uncharacterized including *Spartobacteria*, *Chloroflexi* and *Planctomycetes*. Using an approach that reveals the C assimilation dynamics of specific microbial lineages we describe the ecological properties of functionally defined microbial groups that contribute to decomposition in soil.

stable isotope probing | structure-function relationships | soil microbial ecology | 16S rRNA gene

Abbreviations: C, Carbon; OTU, Operational Taxonomic Unit; SOM, Soil Organic Matter; BD, Buoyand Density; SIP, Stable Isotope Probing

Significance

Soil microorganisms drive C flux through the terrestrial biosphere, and models that predict terrestrial C flux can benefit by accounting for microbial ecophysiology in soils. However, characterizing the ecophysiology of microbes that mediate C decomposition in soil has proven difficult due to their overwhelming diversity. We characterized microbial C metabolism in soil and show that different types of C have distinct decomposition dynamics governed by different microbial lineages. For example, we found that uncharacterized microbial taxa, which are cosmopolitan in soils, assimilated cellulose-C into DNA. These microbes may drive cellulose decomposition on a global scale. We identify microbial lineages engaging in labile and structural C decomposition and explore their ecological properties.

Introduction

Soils worldwide contain 2,300 Pg of carbon (C) which accounts for nearly 80% of the C present in the terrestrial biosphere [1, 2]. C respiration by soil microorganisms produces annually tenfold more CO_2 than fossil fuel emissions [3]. Despite the contribution of microorganisms to global C flux, many global C models ignore the diversity of microbial physiology [4–6] and we still know little about the ecophysiology of soil microorganisms. Such knowledge should assist the development and refinement of global C models [7–10].

Most plant C is comprised of cellulose (30-50%) followed by hemicellulose (20-40%), and lignin (15-

bioRxiv preprint doi: https://doi.org/10.1101/022483; this version posted July 20, 2015. The copyright holder for this preprint (which was not certified by peer review) is the author/funder, who has granted bioRxiv a license to display the preprint in perpetuity. It is made available under aCC-BY-NC-ND 4.0 International license.

25%) [11]. Hemicellulose, being the most soluble, degrades in the early stages of decomposition. Xylans are often an abundant component of hemicellulose, and xylans include differing amounts of xylose, glucose, arabinose, galactose, mannose, and rhamnose [12]. Xylose is often the most abundant sugar in hemicellulose, comprising as much as 60-90% of xylan in some plants (e.g hardwoods [13], wheat [14], and switchgrass [15]). Microbes that respire labile C in the form of sugars proliferate during the initial stages of decomposition [16, 17], and metabolize as much as 75% of sugar C during the first 5 days [18]. In contrast, cellulose decomposition proceeds more slowly with rates increasing for approximately 15 days while degradation continues for 30-90 days [18, 19]. It is hypothesized that different microbial guilds mediate the decomposition of different plant biomass components [19–22]. The degradative succession hypothesis posits that fast growing organisms proliferate in response to the labile fraction of plant biomass such as sugars [23, 24] followed by slow growing organisms targeting structural C such as cellulose [23]. Evidence to support the degradative succession hypothesis comes from observing soil respiration dynamics and characterizing microbes cultured at different stages of decomposition. The degree to which the succession hypothesis presents an accurate model of litter decomposition has been questioned [21, 25, 26] and it's clear that we need new approaches to dissect microbial contributions to C transformations in soils.

Though microorganisms mediate 80-90% of the soil C-cycle [27, 28], and microbial community composition can account for significant variation in C mineralization [29], terrestrial C-cycle models rarely consider the community composition of soils [30, 31]. Rates of soil C transformations are measured without knowledge of the organisms that mediate these reactions [28] leaving the importance of community membership towards maintaining ecosystem function undefined [28, 32, 33]. Variation in microbial community composition can be linked effectively to rates of soil processes when diagnostic genes for specific functions are available (e.g. denitrification [34], nitrification [35–37], methanotrophy [38], and nitrogen fixation [39]). However, the lack of diagnostic genes for describing soil-C transformations has limited progress in characterizing the contributions of individual microbes to decomposition. Remarkably, we still lack basic information on the physiology and ecology of the majority of organisms that live in soils. For example, contributions to soil processes remain uncharacterized for cosmopolitan bacterial phyla in soil such as *Acidobacteria*, *Chloroflexi*, *Planctomycetes*, and *Verrucomicrobia*. These phyla combined can comprise 32% of soil microbial communities (based on surveys of the SSU rRNA genes in soil) [40, 41].

Characterizing the functions of microbial taxa has relied historically on culturing microorganisms and subsequently characterizing their physiology in the laboratory, and on environmental surveys of genes diagnostic for specific processes. But, most microorganisms are difficult to grow in culture [40] and many biogeochemical processes lack suitable diagnostic genes. Nucleic acid stable-isotope probing (SIP) links genetic identity and activity without the need to grow microorganisms in culture and has expanded our knowledge of microbial contributions to biogeochemical processes [42]. However, nucleic acid SIP has notable complications including the need to add large amounts of labeled substrate [43], label dilution resulting in partial labeling of nucleic acids [43–45], the potential for cross-feeding and secondary label incorporation [45–50], and variation in genome G+C content [51–54]. As a result, most applications of SIP have targeted specialized microorganisms such as methanotrophs [43], methanogens [55], syntrophs [56], or microbes that target pollutants [57]. Exploring the soil-C cycle with SIP has proven to be more challenging because SIP has lacked the resolution necessary to characterize the specific contributions of individual microbial groups to the decomposition of plant biomass. High throughput DNA sequencing technology, however, improves the resolving power of SIP [58].

Coupling SIP with high throughput DNA sequencing now enables exploration of microbial C-cycling in soils. SSU rRNA amplicons are readily sequenced from numerous density gradient fractions across multiple samples thereby increasing the resolution of a typical nucleic acid SIP experiment [59]. It is now possible to use far less isotopically labeled substrate resulting in more environmentally realistic experimental conditions [58]. We have employed such a high resolution DNA stable isotope probing approach to explore the assimilation of xylose and/or cellulose into bacterial DNA in an agricultural soil.

Specifically, we added to soil a complex amendment representative of organic matter derived from fresh plant biomass. All treatments received the same amendment but the identity of isotopically labeled substrates was varied between treatments. Specifically, we set up a control treatment where all components were unlabeled, a treatment with ^{13}C-xylose instead of unlabeled xylose, and a treatment with ^{13}C-cellulose instead of unlabeled cellulose. Soil was sampled at days 1, 3, 7, 14, and 30 and we identified microorganisms that assimilated ^{13}C into DNA at each point in time. The experiment was designed to provide a test of the degradative succession hypothesis as it applies to soil bacteria,

bioRxiv preprint doi: https://doi.org/10.1101/022483; this version posted July 20, 2015. The copyright holder for this preprint (which was not certified by peer review) is the author/funder, who has granted bioRxiv a license to display the preprint in perpetuity. It is made available under aCC-BY-NC-ND 4.0 International license.

to identify soil bacteria that metabolize xylose and cellulose, and to characterize temporal dynamics of xylose and cellulose metabolism in soil.

Results

After adding the organic matter amendment to soil, we tracked the flow of ^{13}C from ^{13}C-xylose or ^{13}C-cellulose into microbial DNA over time using DNA-SIP (Figure S1). The amendment consisted of compounds representative of plant biomass including cellulose, lignin, sugars found in hemicellulose, amino acids, and inorganic nutrients (see Supplemental Information (SI)). The amendment was added at 2.9 mg C g^{-1} soil dry weight (d.w.), and this comprised 19% of the total C in the soil. The cellulose-C (0.88 mg C g^{-1} soil d.w.) and xylose-C (0.42 mg C g^{-1} soil d.w.) in the amendment comprised 6% and 3% of the total C in the soil, respectively. The soil microbial community respired 65% of the xylose within one day and 29% of the added xylose remained in the soil at day 30 (Figure S2). In contrast, cellulose-C declined at a rate of approximately 18 μg C d $^{-1}$ g^{-1} soil d.w. and 40% of added cellulose-C remained in the soil at day 30 (Figure S2).

Types of ^{13}C-labeled OTUs changed with time and substrate. We assessed assimilation of ^{13}C into microbial DNA by comparing the SSU rRNA gene sequence composition of SIP density gradient fractions between ^{13}C treatments and the unlabeled control (see Methods and SI). In the gradient density fractions for the control treatment, fraction density represented the majority of the variance in SSU rRNA gene composition (Figure 1). Genome G+C content correlates positively with DNA buoyant density and influences SSU rRNA gene composition in gradient fractions [51]. For the ^{13}C-cellulose treatment, the SSU rRNA gene composition in gradient fractions deviated from control in high density fractions ($>$ 1.72 g mL^{-1}) on days 14 and 30 (Figure 1). For the ^{13}C-xylose treatment, SSU rRNA gene composition in gradient fractions also deviated from control in high density fractions, but it deviated from control on days 1, 3, and 7 (Figure 1). The SSU rRNA gene composition from the ^{13}C-cellulose treatment and ^{13}C-xylose treatment high density gradient fractions differed indicating different microorganisms assimilated C from xylose than cellulose (Figure 1). Further, in the ^{13}C-cellulose treatment, the SSU rRNA gene sequence composition in high density fractions was similar on days 14 and 30 indicating similar microorganisms had ^{13}C-labeled DNA in ^{13}C-cellulose treatments at days 14 and 30. In contrast, in the ^{13}C-xylose treatment, the SSU rRNA gene composition of high density fractions varied between days 1, 3, and 7 indicating that different microbes had ^{13}C-labeled DNA on each of these days. In the ^{13}C-xylose treatment, the SSU gene composition of high density fractions was similar to control on days 14 and 30 (Figure 1) indicating that ^{13}C was no longer detectable in bacterial DNA on these days for this treatment.

Temporal dynamics of OTU relative abundance in experimental soil. We monitored the experimental soil microbial community over the course of the experiment by surveying SSU rRNA genes in non-fractionated DNA from the experimental soil. The SSU rRNA gene composition of the non-fractionated DNA changed with time (Figure S3, P-value = 0.023, R^2 = 0.63, Adonis test [60]). In contrast, the non-fractionated DNA SSU rRNA gene composition showed no statistical evidence for changing with treatment (P-value 0.23, Adonis test) (Figure S3). The latter result demonstrates the substitution of ^{13}C-labeled substrates for unlabeled equivalents could not be shown to alter the soil microbial community composition. Twenty-nine OTUs exhibited sufficient statistical evidence (adjusted P-value $<$0.10, Wald test) to conclude they changed in relative abundance in the non-fractionated DNA over the course of the experiment (Figure S4). When SSU rRNA gene abundances were combined at the taxonomic rank of "class", the classes that changed in abundance (adjusted P-value $<$ 0.10, Wald test) were the *Bacilli* (decreased), *Flavobacteria* (decreased), *Gammaproteobacteria* (decreased), and *Herpetosiphonales* (increased) (Figure S5). Of the 29 OTUs that changed in relative abundance over time, 14 putatively incorporated ^{13}C into DNA (Figure S4). OTUs that likely assimilated ^{13}C from ^{13}C-cellulose into DNA tended to increase in relative abundance with time whereas OTUs that assimilated ^{13}C from ^{13}C-xylose tended to decrease (Figure S6). OTUs that responded to both substrates did not exhibit a consistent relative abundance response over time as a group (Figure S4 and S6).

Changes in the phylogenetic composition of ^{13}C-labeled OTUs with time. If an OTU exhibited strong evidence for assimilating ^{13}C into DNA, we refer to that OTU as a "responder" (see Methods and SI for our operational definition of "responder"). The SSU rRNA gene sequences produced in this study were binned into 5,940 OTUs and we assessed evidence of ^{13}C-labeling from both ^{13}C-cellulose and ^{13}C-xylose for each OTU. Forty-one OTUs responded to ^{13}C-xylose, 55 OTUs responded to ^{13}C-cellulose, and 8 OTUs responded to both xylose and cellulose (Figure 2, Figure 3, Figure S7, Table S1, and Table S2). The number

bioRxiv preprint doi: https://doi.org/10.1101/022483; this version posted July 20, 2015. The copyright holder for this preprint (which was not certified by peer review) is the author/funder, who has granted bioRxiv a license to display the preprint in perpetuity. It is made available under a CC-BY-NC-ND 4.0 International license.

of xylose responders peaked at days 1 and 3 and declined with time. In contrast, the number of cellulose responders increased with time peaking at days 14 and 30 (Figure S8).

The phylogenetic composition of xylose responders changed with time (Figure 2 and Figure 4) and 86% of xylose responders shared > 97% SSU rRNA gene sequence identity with bacteria cultured in isolation (Table S1). On day 1, *Bacilli* OTUs represented 84% of xylose responders (Figure 4) and the majority of these OTUs were closely related to cultured representatives of the genus *Paenibacillus* (Table S1, Figure 3). For example, "OTU.57" (Table S1), annotated as *Paenibacillus*, had a strong signal of ^{13}C-labeling at day 1 coinciding with its maximum relative abundance in non-fractionated DNA. The relative abundance of "OTU.57" declined until day 14 and "OTU.57" did not appear to be ^{13}C-labeled after day 1 (Figure S9). On day 3, *Bacteroidetes* OTUs comprised 63% of xylose responders (Figure 4) and these OTUs were closely related to cultured representatives of the *Flavobacteriales* and *Sphingobacteriales* (Table S1, Figure 3). For example, "OTU.14", annotated as a flavobacterium, had a strong signal for ^{13}C-labeling in the ^{13}C-xylose treatment at days 1 and 3 coinciding with its maximum relative abundance in non-fractionated DNA. The relative abundance of "OTU.14" then declined until day 14 and did not show evidence of ^{13}C-labeling beyond day 3 (Figure S9). Finally, on day 7, *Actinobacteria* OTUs represented 53% of the xylose responders (Figure 4) and these OTUs were closely related to cultured representatives of *Micrococcales* (Table S1, Figure 3). For example, "OTU.4", annotated as *Agromyces*, had signal for ^{13}C-labeling in the ^{13}C-xylose treatment on days 1, 3 and 7 with the strongest evidence of ^{13}C-labeling at day 7 and did not appear ^{13}C-labeled at days 14 and 30. The relative abundance of "OTU.4" in non-fractionated DNA increased until day 3 and then declined until day 30 (Figure S9). *Proteobacteria* were also common among xylose responders at day 7 where they comprised 40% of xylose responder OTUs. Notably, *Proteobacteria* represented the majority (6 of 8) of OTUs that responded to both cellulose and xylose (Figure S7).

The phylogenetic composition of cellulose responders did not change with time to the same extent as the xylose responders. Also, in contrast to xylose responders, cellulose responders often were not closely related (< 97% SSU rRNA gene sequence identity) to cultured isolates. Both the relative abundance and the number of cellulose responders increased over time peaking at days 14 and 30 (Figure 2, Figure S8, and Figure S6). Cellulose responders belonged to the *Proteobacteria* (46%), *Verrucomicrobia* (16%), *Planctomycetes* (16%), *Chloroflexi* (8%), *Bacteroidetes* (8%), *Actinobacteria* (3%), and *Melainabacteria* (1 OTU) (Table S2).

The majority (85%) of cellulose responders outside of the *Proteobacteria* shared < 97% SSU rRNA gene sequence identity to bacteria cultured in isolation. For example, 70% of the *Verrucomicrobia* cellulose responders fell within unidentified *Spartobacteria* clades (Figure 3), and these shared < 85% SSU rRNA gene sequence identity to any characterized isolate. The *Spartobacteria* OTU "OTU.2192" exemplified many cellulose responders (Table S2, Figure S9). "OTU.2192" increased in non-fractionated DNA relative abundance with time and evidence for ^{13}C-labeling of "OTU.2192" in the ^{13}C-cellulose treatment increased over time with the strongest evidence at days 14 and 30 (Figure S9). Most *Chloroflexi* cellulose responders belonged to an unidentified clade within the *Herpetosiphonales* (Figure 3) and they shared < 89% SSU rRNA gene sequence identity to any characterized isolate. Characteristic of *Chloroflexi* cellulose responders, "OTU.64" increased in relative abundance over 30 days and evidence for ^{13}C-labeling of "OTU.64" in the ^{13}C-cellulose treatment peaked days 14 and 30 (Figure S9). *Bacteroidetes* cellulose responders fell within the *Cytophagales* in contrast with *Bacteroidetes* xylose responders that belonged instead to the *Flavobacteriales* or *Sphingobacteriales* (Figure 3). *Bacteroidetes* cellulose responders included one OTU that shared 100% SSU rRNA gene sequence identity to a *Sporocytophaga* species, a genus known to include cellulose degraders. The majority (86%) of cellulose responders in the *Proteobacteria* were closely related (> 97% identity) to bacteria cultured in isolation, including representatives of the genera: *Cellvibrio*, *Devosia*, *Rhizobium*, and *Sorangium*, which are all known for their ability to degrade cellulose (Table S2). Proteobacterial cellulose responders belonged to *Alpha* (13 OTUs), *Beta* (4 OTUs), *Gamma* (5 OTUs), and *Deltaproteobacteria* (6 OTUs).

Characteristics of cellulose and xylose responders. Cellulose responders, relative to xylose responders, tended to have lower relative abundance in non-fractionated DNA, demonstrated signal consistent with higher atom % ^{13}C in labeled DNA, and had lower estimated *rrn* copy number (Figure 5). In the non-fractionated DNA, cellulose responders had lower relative abundance (1.2×10^{-3} (s.d. 3.8×10^{-3})) than xylose responders (3.5×10^{-3} (s.d. 5.2×10^{-3})) (Figure 4, P-value = 1.12×10^{-5}, Wilcoxon Rank Sum test). Six of the ten most common OTUs observed in the non-fractionated DNA responded to xylose, and, seven of the ten most abundant responders to xylose or cellulose in

bioRxiv preprint doi: https://doi.org/10.1101/022483; this version posted July 20, 2015. The copyright holder for this preprint (which was not certified by peer review) is the author/funder, who has granted bioRxiv a license to display the preprint in perpetuity. It is made available under aCC-BY-NC-ND 4.0 International license.

the non-fractionated DNA were xylose responders although "OTU.6" annotated as *Cellvibrio* a cellulose responder at day 14 was the responder found at highest relative abundance (approximately 3% or SSU rRNA genes at day 14, Figure S9).

DNA buoyant density (BD) increases in proportion to atom % ^{13}C. Hence, the extent of ^{13}C incorporation into DNA can be evaluated by the difference in BD between ^{13}C-labeled and unlabeled DNA. We calculated for each OTU its mean BD weighted by relative abundance to determine its "center of mass" within a given density gradient. We then quantified for each OTU the difference in center of mass between control gradients and gradients from ^{13}C-xylose or ^{13}C-cellulose treatments (see SI for the detailed calculation, Figure S11). We refer to the change in center of mass position for an OTU in response to ^{13}C-labeling as $\Delta\hat{BD}$. $\Delta\hat{BD}$ can be used to compare relative differences in ^{13}C-labeling between OTUs. $\Delta\hat{BD}$ values, however, are not comparable to the BD changes observed for DNA from pure cultures both because they are based on relative abundance in density gradient fractions (and not DNA concentration) and because isolated strains grown in uniform conditions generate uniformly labeled molecules while OTUs composed of heterogeneous strains in complex environmental samples do not. Cellulose responder $\Delta\hat{BD}$ (0.0163 g mL^{-1} (s.d. 0.0094)) was greater than that of xylose responders (0.0097 g mL^{-1} (s.d. 0.0094)) (Figure 5, P-value = 1.8610 x 10^{-6}, Wilcoxon Rank Sum test).

We predicted the *rrn* gene copy number for responders as described [61]. The ability to proliferate after rapid nutrient influx correlates positively to a microorganism's *rrn* copy number [62]. Cellulose responders possessed fewer estimated *rrn* copy numbers (2.7 (1.2 s.d.)) than xylose responders (6.2 (3.4 s.d.)) (P = 1.878 x 10^{-9}, Wilcoxon Rank Sum test, Figure 5 and Figure S10). Furthermore, the estimated *rrn* gene copy number for xylose responders was inversely related to the day of first response (P = 2.02 x 10^{-15}, Wilcoxon Rank Sum test, Figure S10,Figure 5).

We assessed phylogenetic clustering of ^{13}C-responsive OTUs with the Nearest Taxon Index (NTI) and the Net Relatedness Index (NRI) [63]. We also quantified the average clade depth of cellulose and xylose responders with the consenTRAIT metric [64]. Briefly, the NRI and NTI evaluate phylogenetic clustering against a null model for the distribution of a trait in a phylogeny. The NRI and NTI values are z-scores or standard deviations from the mean and thus the greater the magnitude of the NRI/NTI, the stronger the evidence for clustering (positive values) or overdispersion (negative values). NRI assesses overall clustering whereas the NTI assesses terminal clustering [65]. The consenTRAIT metric is a measure of the average clade depth for a trait in a phylogenetic tree. NRI values indicate that cellulose responders clustered overall and at the tips of the phylogeny (NRI: 4.49, NTI: 1.43) while xylose responders clustered terminally (NRI: -1.33, NTI: 2.69). The consenTRAIT clade depth for xylose and cellulose responders was 0.012 and 0.028 SSU rRNA gene sequence dissimilarity, respectively. As reference, the average clade depth is approximately 0.017 SSU rRNA gene sequence dissimilarity for arabinase (another five C sugar found in hemicellulose) utilization as inferred from genomic analyses, and was 0.013 and 0.034 SSU rRNA gene sequence dissimilarity for glucosidase and cellulase genomic potential, respectively [64, 66]. These results indicate xylose responders form terminal clusters dispersed throughout the phylogeny while cellulose responders form deep clades of terminally clustered OTUs.

Discussion

We identified microorganisms participating in soil C cycling using a nucleic acid SIP approach. Specifically, we observed assimilation of ^{13}C from either ^{13}C-xylose or ^{13}C-cellulose into DNA for 104 OTUs in an agricultural soil. We found ^{13}C from ^{13}C-xylose appeared to move into and then out of groups of related OTUs over time. By coupling nucleic acid SIP to high throughput sequencing we could diagnose OTU activity even when OTUs were at low relative abundance in non-fractionated DNA (e.g. on three occasions we did not detect ^{13}C-responders in the non-fractionated DNA). Our results support the degradative succession hypothesis, elucidate ecophysiological properties of soil microorganisms, reveal activity of widespread uncultured soil bacteria, and begin to piece together the microbial food web in soils.

The degradative succession hypothesis predicts an ecological transition in activity during the decomposition of labile and structural plant organic matter. Our results concur with the degradative succession hypothesis. Microorganisms consumed xylose-C before cellulose-c and assimilated xylose-C into DNA faster than to cellulose-C. Xylose is a major constituent of hemicellulose and is a labile component of fresh plant biomass. The phylogenetic composition of xylose responders changed between days 1, 3 and 7 and few OTUs appeared ^{13}C-labeled in the ^{13}C-xylose treatment after day 7. In the ^{13}C-cellulose treatment, ^{13}C-labeled OTUs were few in the in the beginning of the experiment but most abundant day 14 and 30. Finally, few (8 of 104) OTUs appeared to metabolize both xylose and cellulose meaning over 30 days cellulose responders grew in succession to xylose responders.

bioRxiv preprint doi: https://doi.org/10.1101/022483; this version posted July 20, 2015. The copyright holder for this preprint (which was not certified by peer review) is the author/funder, who has granted bioRxiv a license to display the preprint in perpetuity. It is made available under a CC-BY-NC-ND 4.0 International license.

Correlations between community composition and environmental characteristics often indirectly reveal microorganisms belonging to ecologically defined groups [67]. In this experiment, we directly identified ecological groups as a function of *in situ* metabolism and inferred the ecological properties of these groups through temporal dynamics of ^{13}C-assimilation, the extent of OTU ^{13}C-labeling, and phylogenetic affiliation. Xylose responders grew faster than cellulose responders and appeared to assimilate C from multiple sources. Xylose responders assimilated xylose-C into DNA within 24 hours and had low $\Delta\hat{BD}$ relative to cellulose responders suggesting xylose was not the sole C source used for growth. Xylose represented 15% of the amendment and 3.5% of total soil C. Xylose responders often included the most abundant OTUs within the non-fractionated DNA and had high estimated *rrn* copy number relative to cellulose responders. However, to some degree, high *rrn* gene copy number may inflate observed xylose responder relative abundance. Notably, the majority of xylose responder SSU rRNA genes (86%) matched SSU rRNA genes from cultured isolates at high sequence identity (> 97%).

Cellulose responders, on the other hand, incorporated ^{13}C into DNA after xylose responders and appeared to specialize in using cellulose as a C source. Cellulose responders grew over a span of weeks and had high $\Delta\hat{BD}$ indicating cellulose remained their dominant C source even though multiple C sources were present (cellulose represented 6% of total C present in soil at the start of the experiment). Cellulose responders were also lower in relative abundance on average within the non-fractionated DNA and had lower estimated *rrn* copy number than xylose responders. The majority of cellulose responders were not close relatives of cultured isolates although a number of cellulose responders shared high SSU rRNA gene sequence identity with cultured *Proteobacteria* (e.g. *Cellvibrio*), . We identified cellulose responders among phyla such as *Verrucomicrobia*, *Chloroflexi*, and *Planctomycetes* – common soil phyla whose functions within soil communities remain unknown.

Verrucomicrobia represented 16% of the cellulose responders. *Verrucomicrobia* are cosmopolitan soil microbes [68] that can make up to 23% of SSU rRNA gene sequences in soils [68] and 9.8% of soil SSU rRNA [69]. Genomic analyses and laboratory experiments show that various isolates within the *Verrucomicrobia* are capable of methanotrophy, diazotrophy, and cellulose degradation [70, 71]. Moreover, *Verrucomicrobia* have been hypothesized to degrade polysaccharides in many environments [72–74]. However, only one of the 15 most abundant verrucomicrobial phylotypes in globally distributed soil samples shared > 93% SSU rRNA gene sequence identity with a cultured isolate [68] and hence the role of soil *Verrucomicrobia* in global C-cycling remains unknown. The majority of verrucomicrobial cellulose responders belonged to two clades that fall within the *Spartobacteria* (Figure 3). *Spartobacteria* outnumbered all other *Verrucomicrobia* phylotypes in SSU rRNA gene surveys of 181 globally distributed soil samples [68]. Given their ubiquity and abundance in soil as well as their demonstrated incorporation of ^{13}C from ^{13}C-cellulose, *Verrucomicrobia* lineages, particularly *Spartobacteria*, may be important contributors to cellulose decomposition on a global scale.

Other notable cellulose responders include OTUs in the *Planctomycetes* and *Chloroflexi* both of which have previously been shown to assimilate ^{13}C from ^{13}C-cellulose added to soil [75]. *Planctomycetes* are common in soil [40], comprising 4 to 7% of bacterial cells in many soils [76, 77] and 7% ± 5% of SSU rRNA [78]. Although soil *Planctomycetes* are widespread, their activities in soil remain uncharacterized. *Plantomycetes* represented 16% of cellulose responders and shared < 92% SSU rRNA gene sequence identity to their most closely related cultured isolates. *Chloroflexi* are known for metabolically dynamic lifestyles ranging from anoxygenic phototrophy to organohalide respiration [79] and are among the six most abundant bacterial phyla in soil [40]. Recent studies have focused on *Chloroflexi* roles in C cycling [79–81] and several *Chloroflexi* isolates use cellulose [79–81]. Four of the five *Chloroflexi* cellulose responders belong to a single clade within the *Herpetosiphonales* (Figure 3).

Finally, a single cellulose responder belonged to the *Melainabacteria* phylum (95% shared SSU rRNA gene sequence identity with *Vampirovibrio chlorellavorus*). The phylogenetic position of *Melainabacteria* is debated but *Melainabacteria* have been proposed to be a non-phototrophic sister phylum to *Cyanobacteria*. An analysis of a *Melainabacteria* genome [82] suggests the genomic capacity to degrade polysaccharides though *Vampirovibrio chlorellavorus* is an obligate predator of green alga [83].

Responders did not necessarily assimilate ^{13}C directly from ^{13}C-xylose or ^{13}C-cellulose. In many ways, knowledge of secondary C degradation and/or microbial biomass turnover may be more interesting with respect to the soil C-cycle than knowledge of primary degradation. The response to xylose suggests xylose-C moved through different trophic levels within the soil bacterial food web. The *Bacilli* degraded xylose first (65% of the xylose-C had been respired by day 1) representing 84% of day 1 xylose responders. *Bacilli* also comprised about 6% of SSU rRNA genes present

bioRxiv preprint doi: https://doi.org/10.1101/022483; this version posted July 20, 2015. The copyright holder for this preprint (which was not certified by peer review) is the author/funder, who has granted bioRxiv a license to display the preprint in perpetuity. It is made available under a CC-BY-NC-ND 4.0 International license.

in non-fractionated DNA on day 1. However, few *Bacilli* remained ^{13}C-labeled by day 3 and their abundance declined reaching about 2% of soil SSU rRNA genes by day 30. Members of the *Bacillus* [84] and *Paenibacillus* in particular [59] have been previously implicated as labile C decomposers. The decline in relative abundance of *Bacilli* could be attributed to mortality and/or sporulation coupled to mother cell lysis. *Bacteroidetes* OTUs appeared ^{13}C-labeled at day 3 concomitant with the decline in relative abundance and loss of ^{13}C-label for *Bacilli*. Finally, *Actinobacteria* appeared ^{13}C-labeled at day 7 as *Bacteroidetes* xylose responders declined in relative abundance and became unlabeled. Hence, it seems reasonable to propose that *Bacteroidetes* and *Actinobacteria* xylose responders became labeled via the consumption of ^{13}C derived from ^{13}C-labeled microbial biomass as opposed to primary degradation of ^{13}C-xylose.

The inferred physiology of *Actinobacteria* and *Bacteroidetes* xylose responders provides further evidence for C transfer by saprotrophy and/or predation. Most of the *Actinobacteria* xylose responders that appeared ^{13}C-labeled at day 7 were members of the *Micrococcales* (Figure 3) and the most abundant ^{13}C-labeled *Micrococcales* OTU at day 7 (OTU.4, Table S1) is annotated as belonging in the *Agromyces*. *Agromyces* are facultative predators that feed on the gram-positive *Luteobacter* in culture [85]. Additionally, certain types of *Bacteroidetes* can assimilate ^{13}C from ^{13}C-labeled *Escherichia coli* added to soil [86]. Alternatively, it is possible that *Bacilli*, *Bacteroidetes*, and *Actinobacteria* are adapted to use xylose at different concentrations and that the observed activity dynamics resulted from changes in xylose concentration over time and/or that *Actinobacteria* and *Bacteroidetes* xylose responders consumed waste products generated by primary xylose metabolism (e.g. organic acids produced during xylose metabolism). These latter two hypotheses cannot explain the sequential loss of ^{13}C-label, however. If trophic transfer caused the activity dynamics, at least three different ecological groups exchanged C in 7 days. Models of the soil C cycle often exclude trophic interactions between soil bacteria (e.g. [87]), yet when soil C models do account for predators and/or saprophytes, trophic interactions are predicted to have significant effects on the fate of soil C [88].

Implications for soil C cycling models. Functional niche characterization for soil microorganisms is necessary to predict whether and how biogeochemical processes vary with microbial community composition. Functional niches are defined by soil microbiologists and have been successfully incorporated into biogeochemical process models (E.g. [88, 89]). In some C models ecological strategies such as growth rate and substrate specificity are parameters for functional niche behavior [88]. The phylogenetic breadth of a functionally defined group is often inferred from the distribution of diagnostic genes across genomes [66] or from the physiology of isolates cultured on laboratory media [64]. For instance, the wide distribution of the glycolysis operon in microbial genomes is interpreted as evidence that many soil microorganisms participate in glucose turnover [9]. However, the functional niche may depend less on the distribution of diagnostic genes across genomes and more on life history traits that allow organisms to compete for a given substrate as it occurs in the soil. For instance, fast growth and rapid resuscitation allow microorganisms to compete for labile C which may often be transient in soil. Hence, life history traits may constrain the diversity of microbes that metabolize a given C source in the soil under a given set of conditions.

Biogeochemical processes mediated by a broad array of taxa are assumed to be insensitive to community change whereas community change is assumed to affect processes mediated by a narrow suite of microorganisms [9, 90]. In addition, the diversity of a functionally defined group engaged in a specific C transformation is expected to correlate positively with C lability [9]. However, the diversity of labile C and structural C decomposers in soil has not been quantified directly. We found comparable numbers of OTUs responded to ^{13}C-cellulose and ^{13}C-xylose (63 and 49, respectively). Cellulose responders were phylogenetically clustered suggesting that the ability to degrade cellulose is phylogenetically conserved. The clade depth of cellulose responders, 0.028 SSU rRNA gene sequence dissimilarity, is on the same order as that observed for glycoside hydrolases which are diagnostic enzymes for cellulose degradation [66]. Xylose responders clustered in terminal branches indicating groups of closely related taxa metabolized xylose but xylose responders also clustered phylogenetically with respect to time of response (Figure 3, Figure 4). For example, xylose responders on day 1 are dominated by members of *Paenibacillus*. Thus, microorganisms that degraded labile C and structural C were both limited in diversity. Although the genes for xylose metabolism are likely widespread in the soil community, it's possible only a limited diversity of organisms had the ecological characteristics required to degrade xylose under experimental conditions. Therefore it's possible that only a limited number of taxa actually participate in the metabolism of labile C-sources under a given set of conditions, and hence changes in community composition may alter the dynamics of structural *and* labile C-transformations in soil.

bioRxiv preprint doi: https://doi.org/10.1101/022483; this version posted July 20, 2015. The copyright holder for this preprint (which was not certified by peer review) is the author/funder, who has granted bioRxiv a license to display the preprint in perpetuity. It is made available under aCC-BY-NC-ND 4.0 International license.

Broadly, we observed labile C use by fast growing generalists and structural C use by slow growing specialists. These results agree with the MIMICS model which simulates leaf litter decomposition by modeling microbial decomposers as two functionally defined groups, copiotrophs or oligotrophs [89]. Including these functional types improved predictions of C storage in response to environmental change relative to models that did not consider any microbial physiological diversity. We identified microbial lineages engaged in labile and structural C decomposition that can be defined as copiotrophs or oligotrophs, respectively. We also observed rate differences in turnover of xylose responder biomass relative to cellulose responders which may be important to consider when modeling microbial turnover input to SOM. It's also clear that the characterization of microbes as copiotrophs and oligotrophs may miss other, vital functional types mediating C-cycling in soil. That is, soil-C may travel through multiple bacterial trophic levels where each C transfer represents an opportunity for C stabilization in association with soil minerals or C loss by respiration. Our understanding of soil C dynamics will likely improve as we develop a more granular understanding of the ecological diversity of microorganisms that mediate C transformations in soil.

Conclusion. Microorganisms govern C-transformations in soil influencing climate change on a global scale but we do not know the identities of microorganisms that carry out specific transformations. In this experiment microbes from physiologically uncharacterized but cosmopolitan soil lineages participated in cellulose decomposition. Cellulose responders included members of the *Verrucomicrobia* (*Spartobacteria*), *Chloroflexi*, *Bacteroidetes* and *Planctomycetes*. *Spartobacteria* in particular are globally cosmopolitan soil microorganisms and are often the most abundant *Verrucomicrobia* order in soil [68]. Fast-growing aerobic spore formers from *Firmicutes* assimilated labile C in the form of xylose. Xylose responders within the *Bacteroidetes* and *Actinobacteria* likely became labeled by consuming ^{13}C-labeled constituents of microbial biomass either by saprotrophy or predation. Our results suggest that cosmopolitan *Spartobacteria* may degrade cellulose on a global scale, plant C may travel through a trophic cascade within the bacterial food web after primary decomposition, and life history traits may act as a filter constraining the diversity of active microorganisms relative to those with the genomic potential for a given metabolism.

Methods

All code to take raw SSU rRNA gene sequencing reads to final publication figures and through all presented analyses is located at the following URL: `https://github.com/chuckpr/CSIP_succession_data_analysis`.
DNA sequences are deposited on MG-RAST (Accession XXXXXXX).

Twelve soil cores (5 cm diameter x 10 cm depth) were collected from six sampling locations within an organically managed agricultural field in Penn Yan, New York. Soils were sieved (2 mm), homogenized, distributed into flasks (10 g in each 250 ml flask, n = 36) and equilibrated for 2 weeks. We amended soils with a mixture containing 2.9 mg C g^{-1} soil dry weight (d.w.) and brought experimental soil to 50% water holding capacity. By mass the amendment contained 38% cellulose, 23% lignin, 20% xylose, 3% arabinose, 1% galactose, 1% glucose, and 0.5% mannose. 10.6% amino acids (Teknova C9795) and 2.9% Murashige Skoog basal salt mixture which contains macro and micro-nutrients that are associated with plant biomass (Sigma Aldrich M5524). This mixture approximates the molecular composition of switchgrass biomass with hemicellulose replaced by its constituent monomers [91]. We set up three parallel treatments varying the isotopically labeled component in each treatment. The treatments were (1) a control treatment with all unlabeled components, (2) a treatment with ^{13}C-cellulose instead of unlabeled cellulose (synthesized as described in SI), and (3) a treatment with ^{13}C-xylose (98 atom% ^{13}C, Sigma Aldrich) instead of unlabeled xylose. Other details relating to substrate addition can be found in SI. Microcosms were sampled destructively at days 1 (control and xylose only), 3, 7, 14, and 30 and soils were stored at -80°C until nucleic acid extraction. The abbreviation 13CXPS refers to the ^{13}C-xylose treatment (^{13}C Xylose Plant Simulant), 13CCPS refers to the ^{13}C-cellulose treatment, and 12CCPS refers to the control treatment.

We used DESeq2 (R package), an RNA-Seq differential expression statistical framework [92], to identify OTUs that were enriched in high density gradient fractions from ^{13}C-treatments relative to corresponding gradient fractions from control treatments (for review of RNA-Seq differential expression statistics applied to microbiome OTU count data see (30)). We define "high density gradient fractions" as gradient fractions whose density falls between 1.7125 and 1.755 g ml^{-1}. Briefly, DESeq2 includes several features that enable robust estimates of standard error in addition to reliable ranking of logarithmic fold change (LFC) (i.e. gamma-Poisson regression coefficients) in OTU relative abundance even with low count OTUs where LFC can often be noisy. Further, statistical evalu-

bioRxiv preprint doi: https://doi.org/10.1101/022483; this version posted July 20, 2015. The copyright holder for this preprint (which was not certified by peer review) is the author/funder, who has granted bioRxiv a license to display the preprint in perpetuity. It is made available under aCC-BY-NC-ND 4.0 International license.

ation of LFC can be performed with user-selected thresholds as opposed to the typical null hypothesis that LFC is exactly zero enabling the most biologically interesting OTUs to be identified for subsequent analyses. For each OTU, we calculated LFC and corresponding standard errors for enrichment in high density gradient fractions of ^{13}C treatments relative to control. Subsequently, a one-sided Wald test was used to statistically assess LFC values. The user-defined null hypothesis was that LFC was less than one standard deviation above the mean of all LFC values. P-values were corrected for multiple comparisons using the Benjamini and Hochberg method [93]. We independently filtered OTUs on the basis of sparsity prior to correcting P-values for multiple comparisons. The sparsity value that yielded the most adjusted P-values less than 0.10 was selected for independent filtering by sparsity. Briefly, OTUs were eliminated if they failed to appear in at least 45% of high density gradient fractions for a given ^{13}C/control treatment pair. These sparse OTUs are unlikely to have sufficient data to allow for the determination of statistical significance. We selected a false discovery rate of 10% to denote statistical significance.

See SI for additional information on experimental and analytical methods.

Acknowledgements. The authors would like to acknowledge the assistance of John Christian Gaby and Mallory Choudoir in developing the method used to produce ^{13}C-labeled cellulose. We would also like to thank Steve Zinder, Nelson Hairston, and Nick Youngblut for providing comments that were helpful in the development of this manuscript. This material is based upon work supported by the Department of Energy Office of Science, Office of Biological & Environmental Research Genomic Science Program under Award Numbers DE-SC0004486 and DE-SC0010558.

References

1. Amundson R (2001) The carbon budget in soils. *Annu Rev Earth Planet Sci* 29(1): 535–562.
2. Batjes N-H (1996) Total carbon and nitrogen in the soils of the world. *Eur J Soil Sci* 47(2): 151–163.
3. Chapin F (2002) Principles of terrestrial ecosystem ecology. (Springer, New York)
4. Allison S-D, Wallenstein M-D, Bradford M-A (2010) Soil-carbon response to warming dependent on microbial physiology. *Nat Geosci* 3(5): 336–340.
5. Six J, Frey S-D, Thiet R-K, Batten K-M (2006) Bacterial and fungal contributions to carbon sequestration in agroecosystems. *Soil Sci Soc Am J* 70(2): 555.
6. Treseder K-K, Balser T-C, Bradford M-A, Brodie E-L, Dubinsky E-A, Eviner V-T, *et al.* (2011) Integrating microbial ecology into ecosystem models: challenges and priorities. *Biogeochemistry* 109(1-3): 7–18.
7. Bradford M-A, Fierer N, Reynolds J-F (2008) Soil carbon stocks in experimental mesocosms are dependent on the rate of labile carbon, nitrogen and phosphorus inputs to soils. *Funct Ecol* 22(6): 964–974.
8. Neff J-C, Asner G-P (2001) Dissolved organic carbon in terrestrial ecosystems: synthesis and a model. *Ecosystems* 4(1): 29–48.
9. McGuire K-L, Treseder K-K (2010) Microbial communities and their relevance for ecosystem models: Decomposition as a case study. *Soil Biol Biochem* 42(4): 529–535.
10. Wieder W-R, Bonan G-B, Allison S-D (2013) Global soil carbon projections are improved by modelling microbial processes. *Nat Clim Chang* 3(10): 909–912.
11. Lynd L-R, Weimer P-J, van Zyl W-H, Pretorius I-S (2002) Microbial cellulose utilization: fundamentals and biotechnology. *Microbiology and molecular biology reviews* 66(3): 506–table of contents.
12. Saha B-C (2003) Hemicellulose bioconversion. *J Ind Microbiol Biotechnol* 30(5): 279–291.
13. Spiridon I, Popa V-I (2008) Chapter 13 - Hemicelluloses: Major Sources, Properties and Applications. *Monomers, Polymers and Composites from Renewable Resources*, , eds. Belgacem M-N, Gandini A (Elsevier, New York), pp 289–304.
14. Sun X-F, Xu F, Zhao H, Sun R-C, Fowler P, Baird M-S (2005) Physicochemical characterisation of residual hemicelluloses isolated with cyanamide-activated hydrogen peroxide from organosolv pre-treated wheat straw. *Bioresour Technol* 96(12): 1342–1349.
15. Bunnell K, Rich A, Luckett C, Wang Y-J, Martin E, Carrier D-J (2013) Plant maturity effects on the physicochemical properties and dilute acid hydrolysis of switchgrass (panicum virgatum, l.) hemicelluloses. *ACS Sustain Chem Eng* 1(6): 649–654.
16. Garrett S-D (1951) Ecological groups of soil fungi: a survey of substrate relationships. *New Phytol* 50(2): 149–166.
17. Alexander M (1964) Biochemical ecology of soil microorganisms. *Annual Rev Microbiol* 18(1): 217–250.
18. Engelking B, Flessa H, Joergensen R-G (2007) Microbial use of maize cellulose and sugarcane sucrose monitored by changes in the 13C/12C ratio. *Soil Biol Biochem* 39(8): 1888–1896.
19. Hu S, van Bruggen A-HC (1997) Microbial dynamics associated with multiphasic decomposition of 14c-labeled cellulose in soil. *Microb Ecol* 33(2): 134–143.
20. Rui J, Peng J, Lu Y (2009) Succession of bacterial populations during plant residue decomposition in rice field soil. *Appl Environ Microbiol* 75(14): 4879–4886.
21. Kjöller A-H, Struwe S (2002) Fungal Communities, Succession, Enzymes, and Decomposition. *Enzymes in the Environment*, Books in Soils, Plants, and the Environment (Marcel Dekker, New York), pp 306–324.
22. Bastian F, Bouziri L, Nicolardot B, Ranjard L (2009) Impact of wheat straw decomposition on successional patterns of soil microbial community structure. *Soil Biol Biochem* 41(2): 262–275.
23. Garrett S-D (1963) Soil Fungi and soil fertility. (Pergamon Press, New York)
24. Bremer E, Kuikman P (1994) Microbial utilization of 14C[U]glucose in soil is affected by the amount and timing of glucose additions. *Soil Biol Biochem* 26(4): 511–517.
25. Frankland J-C (1998) Fungal succession – unravelling the unpredictable. *Mycol Res* 102(1): 1–15.
26. Osono T (2005) Colonization and succession of fungi during decomposition of Swida controversa leaf litter. *Mycologia* 97(3): 589–597.
27. Coleman D-C, Crossley D-A (1996) fundamentals of soil ecology. (Academic Press, Waltham, Massachusetts)
28. Nannipieri P, Ascher J, Ceccherini M-T, Landi L, Pietramellara G, Renella G (2003) Microbial diversity and soil functions. *Eur J Soil Sci* 54(4): 655–670.
29. Strickland M-S, Lauber C, Fierer N, Bradford M-A (2009) Testing the functional significance of microbial community composition. *Ecology* 90(2): 441–451.
30. Zak D-R, Blackwood C-B, Waldrop M-P (2006) A molecular dawn for biogeochemistry. *Trends Ecol Evol* 21(6): 288–295.
31. Reed H-E, Martiny J-BH (2007) Testing the functional significance of microbial composition in natural communities. *FEMS Microbiol Ecol* 62(2): 161–170.
32. Schimel J-P, Schaeffer S-M (2012) Microbial control over carbon cycling in soil. *Front Microbiol* 3: 348. doi: 10.3389/fmicb.2012.00348
33. Allison S-D, Martiny J-BH (2008) Resistance resilience, and redundancy in microbial communities. *Proc Natl Acad Sci USA* 105(Supplement 1): 11512–11519.

bioRxiv preprint doi: https://doi.org/10.1101/022483; this version posted July 20, 2015. The copyright holder for this preprint (which was not certified by peer review) is the author/funder, who has granted bioRxiv a license to display the preprint in perpetuity. It is made available under a CC-BY-NC-ND 4.0 International license.

34. Cavigelli M-A, Robertson G-P (2000) The functional significance of denitrifier community composition in a terrestrial ecosystem. *Ecology* 81(5): 1402–1414.
35. Carney K-M, Matson P-A, Bohannan B-JM (2004) Diversity and composition of tropical soil nitrifiers across a plant diversity gradient and among land-use types. *Ecol Lett* 7(8): 684–694.
36. Hawkes C-V, Wren I-F, Herman D-J, Firestone M-K (2005) Plant invasion alters nitrogen cycling by modifying the soil nitrifying community. *Ecol Lett* 8(9): 976–985.
37. Webster G, Embley T-M, Freitag T-E, Smith Z, Prosser J-I (2005) Links between ammonia oxidizer species composition, functional diversity and nitrification kinetics in grassland soils. *Environ Microbiol* 7(5): 676–684.
38. Gulledge J, Doyle A-P, Schimel J-P (1997) Different NH4+-inhibition patterns of soil CH4 consumption: A result of distinct CH4-oxidizer populations across sites? *Soil Biol Biochem* 29(1): 13–21.
39. Hsu S-F, Buckley D-H (2009) Evidence for the functional significance of diazotroph community structure in soil. *ISME J* 3(1): 124–136.
40. Janssen P-H (2006) Identifying the dominant soil bacterial taxa in libraries of 16S rRNA and 16S rRNA genes. *Appl Environ Microbiol* 72(3): 1719–1728.
41. Buckley D-H, Schmidt T-M (2002) Exploring the diversity of soil - a microbial rainforest. *Biodiversity of Microbial Life: Foundation of Earth's Biosphere*, , ed. Reysenbach A-L (Wiley, New York, New York, USA), pp 183–208.
42. Chen Y, Murrell J-C (2010) When metagenomics meets stable-isotope probing: progress and perspectives. *Trends Microbiol* 18(4): 157–163.
43. Radajewski S, Ineson P, Parekh N-R, Murrell J-C (2000) Stable-isotope probing as a tool in microbial ecology. *Nature* 403(6770): 646–649.
44. Manefield M, Whiteley A-S, Griffiths R-I, Bailey M-J (2002) RNA Stable isotope probing a novel means of linking microbial community function to phylogeny. *Appl Environ Microbiol* 68(11): 5367–5373.
45. McDonald I-R, Radajewski S, Murrell J-C (2005) Stable isotope probing of nucleic acids in methanotrophs and methylotrophs: A review. *Org Geochem* 36(5): 779–787.
46. Morris S-A, Radajewski S, Willison T-W, Murrell J-C (2002) Identification of the functionally active methanotroph population in a peat soil microcosm by stable-isotope probing. *Appl Environ Microbiol* 68(3): 1446–1453.
47. Hutchens E, Radajewski S, Dumont M-G, McDonald I-R, Murrell J-C (2004) Analysis of methanotrophic bacteria in Movile Cave by stable isotope probing. *Environ Microbiol* 6(2): 111–120.
48. Lueders T, Manefield M, Friedrich M (2004) Enhanced sensitivity of DNA- and rRNA-based stable isotope probing by fractionation and quantitative analysis of isopycnic centrifugation gradients.. *Environ Microbiol* 6: 73–8.
49. DeRito C-M, Pumphrey G-M, Madsen E-L (2005) Use of field-based stable isotope probing to identify adapted populations and track carbon flow through a phenol-degrading soil microbial community. *Appl Environ Microbiol* 71(12): 7858–7865.
50. Ziegler S-E, White P-M, Wolf D-C, Thoma G-J (2005) Tracking the fate and recycling of ^{13}C-labeled glucose in soil. *Soil Sci* 170(10): 767–778.
51. Buckley D-H, Huangyutitham V, Hsu S-F, Nelson T-A (2007) Stable isotope probing with ^{15}N achieved by disentangling the effects of genome G+C content and isotope enrichment on DNA density. *Appl Environ Microbiol* 73(10): 3189–3195.
52. Birnie G-D (1978) Centrifugal separations in Molecular and cell biology. (Butterworth & Co Publishers Ltd, Boston)
53. Holben W-E, Harris D (1995) DNA-based monitoring of total bacterial community structure in environmental samples. *Molecular Ecology* 4(5): 627–632.
54. Nüsslein K, Tiedje J-M (1999) Soil bacterial community shift correlated with change from forest to pasture vegetation in a tropical soil. *Appl Environ Microbiol* 65(8): 3622–3626.
55. Lu Y, Conrad R (2005) In situ stable isotope probing of methanogenic archaea in the rice rhizosphere. *Science* 309(5737): 1088–1090.
56. Lueders T, Pommerenke B, Friedrich M-W (2004) Stable-isotope probing of microorganisms thriving at thermodynamic limits: syntrophic propionate oxidation in flooded soil. *Appl Environ Microbiol* 70(10): 5778–5786.
57. DeRito C-M, Pumphrey G-M, Madsen E-L (2005) Use of field-based stable isotope probing to identify adapted populations and track carbon flow through a phenol-degrading soil microbial community. *Appl Environ Microbiol* 71(12): 7858–7865.
58. Aoyagi T, Hanada S, Itoh H, Sato Y, Ogata A, Friedrich M-W, *et al.* (2015) Ultra-high-sensitivity stable-isotope probing of rRNA by high-throughput sequencing of isopycnic centrifugation gradients. *Environ Microbiol Rep* 7(2): 282–287.
59. Verastegui Y, Cheng J, Engel K, Kolczynski D, Mortimer S, Lavigne J, *et al.* (2014) Multisubstrate isotope labeling and metagenomic analysis of active soil bacterial communities. *mBio* 5(4): e01157–14.
60. Anderson M-J (2001) A new method for non-parametric multivariate analysis of variance. *Austral Ecol* 26(1): 32–46.
61. Kembel S-W, Wu M, Eisen J-A, Green J-L (2012) Incorporating 16S gene copy number information improves estimates of microbial diversity and abundance. *PLoS Comput Biol* 8(10): e1002743.
62. Klappenbach J-A, Dunbar J-M, Schmidt T-M (2000) rRNA Operon copy number reflects ecological strategies of bacteria. *Appl Environ Microbiol* 66(4): 1328–1333.
63. Webb C-O (2000) Exploring the phylogenetic structure of ecological communities: an example for rain forest trees.. *Am Nat* 156(2): 145–155.
64. Martiny A-C, Treseder K, Pusch G (2013) Phylogenetic conservatism of functional traits in microorganisms. *ISME J* 7(4): 830–838.
65. Evans S-E, Wallenstein M-D (2014) Climate change alters ecological strategies of soil bacteria. *Ecol Lett* 17(2): 155–164.
66. Berlemont R, Martiny A-C (2013) Phylogenetic distribution of potential cellulases in bacteria. *Appl Environ Microbiol* 79(5): 1545–1554.
67. Fierer N, Bradford M-A, Jackson R-B (2007) Toward an ecological classification of soil bacteria. *Ecology* 88(6): 1354–1364.
68. Bergmann G-T, Bates S-T, Eilers K-G, Lauber C-L, Caporaso J-G, Walters W-A, *et al.* (2011) The under-recognized dominance of Verrucomicrobia in soil bacterial communities. *Soil Biol Biochem* 43(7): 1450–1455.
69. Buckley D-H, Schmidt T-M (2001) Environmental factors influencing the distribution of rRNA from Verrucomicrobia in soil. *FEMS Microbiol Ecol* 35(1): 105–112.
70. Wertz J-T, Kim E, Breznak J-A, Schmidt T-M, Rodrigues J-LM (2011) Genomic and physiological characterization of the Verrucomicrobia isolate diplosphaera colitermitum gen. nov. sp. nov., reveals microaerophily and nitrogen fixation genes. *Appl Environ Microbiol* 78(5): 1544–1555.
71. Otsuka S, Ueda H, Suenaga T, Uchino Y, Hamada M, Yokota A, *et al.* (2012) Roseimicrobium gellanilyticum gen. nov. sp. nov., a new member of the class Verrucomicrobiae. *Int J Syst Evol Microbiol* 63(Pt 6): 1982–1986.
72. Fierer N, Ladau J, Clemente J-C, Leff J-W, Owens S-M, Pollard K-S, *et al.* (2013) Reconstructing the microbial diversity and function of pre-agricultural tallgrass prairie soils in the united states. *Science* 342(6158): 621–624.
73. Chin K-J, Hahn D, Hengstmann U, Liesack W, Janssen P-H (1999) Characterization and identification of numerically abundant culturable bacteria from the anoxic bulk soil of rice paddy microcosms. *Appl Environ Microbiol* 65(11): 5042–5049.
74. Herlemann D-PR, Lundin D, Labrenz M, Jurgens K, Zheng Z, Aspeborg H, *et al.* (2013) Metagenomic de novo assembly of an aquatic representative of the verrucomicrobial class spartobacteria. *mBio* 4(3): e0056912.
75. Schellenberger S, Kolb S, Drake H-L (2010) Metabolic responses of novel cellulolytic and saccharolytic agricultural soil Bacteria to oxygen. *Environ Microbiol* 12(4): 845–861.
76. Zarda B, Hahn D, Chatzinotas A, Schnhuber W, Neef A, Amann R-I, *et al.* (1997) Analysis of bacterial community structure in bulk soil by in situ hybridization. *Arch Microbiol* 168(3): 185–192.
77. Chatzinotas A, Sandaa R-A, Schnhuber W, Amann R, Daae F-L, Torsvik V, *et al.* (1998) Analysis of broad-scale differences in microbial community composition of two pristine forest soils. *Syst Appl Microbiol* 21(4): 579–587.
78. Buckley D-H, Schmidt T-M (2003) Diversity and dynamics of microbial communities in soils from agro-ecosystems. *Environ Microbiol* 5(6): 441–452.

bioRxiv preprint doi: https://doi.org/10.1101/022483; this version posted July 20, 2015. The copyright holder for this preprint (which was not certified by peer review) is the author/funder, who has granted bioRxiv a license to display the preprint in perpetuity. It is made available under a CC-BY-NC-ND 4.0 International license.

79. Hug L-A, Castelle C-J, Wrighton K-C, Thomas B-C, Sharon I, Frischkorn K-R, *et al.* (2013) Community genomic analyses constrain the distribution of metabolic traits across the Chloroflexi phylum and indicate roles in sediment carbon cycling. *Microbiome* 1(1): 22.
80. Goldfarb K-C, Karaoz U, Hanson C-A, Santee C-A, Bradford M-A, Treseder K-K, *et al.* (2011) Differential growth responses of soil bacterial taxa to carbon substrates of varying chemical recalcitrance. *Front Microbiol* 2: 94. doi: 10.3389/fmicb.2011.00094
81. Cole J-K, Gieler B-A, Heisler D-L, Palisoc M-M, Williams A-J, Dohnalkova A-C, *et al.* (2013) Kallotenue papyrolyticum gen. nov. sp. nov., a cellulolytic and filamentous thermophile that represents a novel lineage (Kallotenuales ord. nov., Kallotenuaceae fam. nov.) within the class Chloroflexia. *Int J Syst Evol Microbiol* 63(Pt 12): 4675–4682.
82. Rienzi S-CD, Sharon I, Wrighton K-C, Koren O, Hug L-A, Thomas B-C, *et al.* (2013) The human gut and groundwater harbor non-photosynthetic bacteria belonging to a new candidate phylum sibling to Cyanobacteria. *eLIFE* 2: e01102.
83. Gromov B-V, Mamkaeva K-A (1972) [Electron microscopic study of parasitism by Bdellovibrio chlorellavorus bacteria on cells of the green alga Chlorella vulgaris]. *Tsitologiia* 14(2): 256–260.
84. Cleveland C-C, Nemergut D-R, Schmidt S-K, Townsend A-R (2007) Increases in soil respiration following labile carbon additions linked to rapid shifts in soil microbial community composition. *Biogeochemistry* 82(3): 229–240.
85. Casida L-E (1983) Interaction of *Agromyces* ramosus with other bacteria in soil.. *Appl Environ Microbiol* 46(4): 881–888.
86. Lueders T, Kindler R, Miltner A, Friedrich M-W, Kaestner M (2006) Identification of bacterial micropredators distinctively active in a soil microbial food web. *Appl Environ Microbiol* 72(8): 5342–5348.
87. Moore J-C, Walter D-E, Hunt H-W (1988) Arthropod regulation of micro- and mesobiota in below-ground detrital food webs. *Annu Rev Entomol* 33(1): 419–435.
88. Kaiser C, Franklin O, Dieckmann U, Richter A (2014) Microbial community dynamics alleviate stoichiometric constraints during litter decay. *Ecol Lett* 17(6): 680–690.
89. Wieder W-R, Grandy A-S, Kallenbach C-M, Bonan G-B (2014) Integrating microbial physiology and physiochemical principles in soils with the MIcrobial-MIneral Carbon Stabilization (MIMICS) model. *Biogeosciences* 11(14): 3899–3917.
90. Schimel J (1995) Ecosystem consequences of microbial diversity and community structure. *Arctic and alpine biodiversity: patterns, causes and ecosystem consequences*, , eds. Chapin III F-S, Korner C, Ecological Studies (Springer, Berlin Heidelberg), pp 239–254.
91. Schneckenberger K, Demin D, Stahr K, Kuzyakov Y (2008) Microbial utilization and mineralization of ^{14}C glucose added in six orders of concentration to soil. *Soil Biol Biochem* 40(8): 1981–1988.
92. Love M-I, Huber W, Anders S (2014) Moderated estimation of fold change and dispersion for RNA-seq data with DESeq2. *Genome Biol* 15(12): 550.
93. Benjamini Y, Hochberg Y (1995) Controlling the false discovery rate: A practical and powerful approach to multiple testing. *Journal of the Royal Statistical Society. Series B (Methodological)* 57(1): 289–300.

bioRxiv preprint doi: https://doi.org/10.1101/022483; this version posted July 20, 2015. The copyright holder for this preprint (which was not certified by peer review) is the author/funder, who has granted bioRxiv a license to display the preprint in perpetuity. It is made available under a CC-BY-NC-ND 4.0 International license.

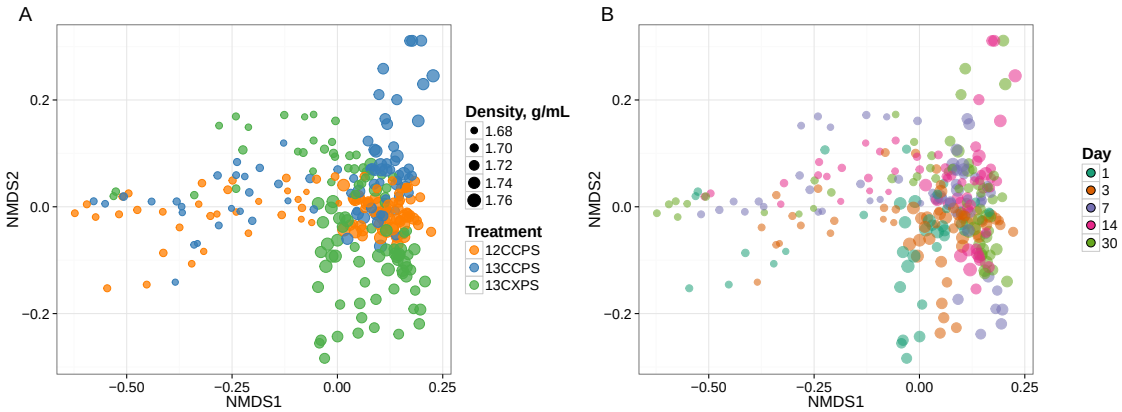

Fig. 1. NMDS analysis of SIP gradient fraction SSU rRNA gene sequence composition reveals differences in the sequence composition of gradient fractions is correlated to fraction density, isotopic labeling, and time. SSU rRNA gene compositon was profiled for fractions for each density gradient. ^{13}C-labeling of DNA is apparent because the SSU rRNA gene composition of gradient fractions from ^{13}C and control treatments differ at high density. Each point on the NMDS plot represents one gradient fraction. SSU rRNA gene composition differences between gradient fractions were quantified by the weighted Unifrac metric. The size of each point is positively correlated with density and colors indicate the treatment (A) or day (B).

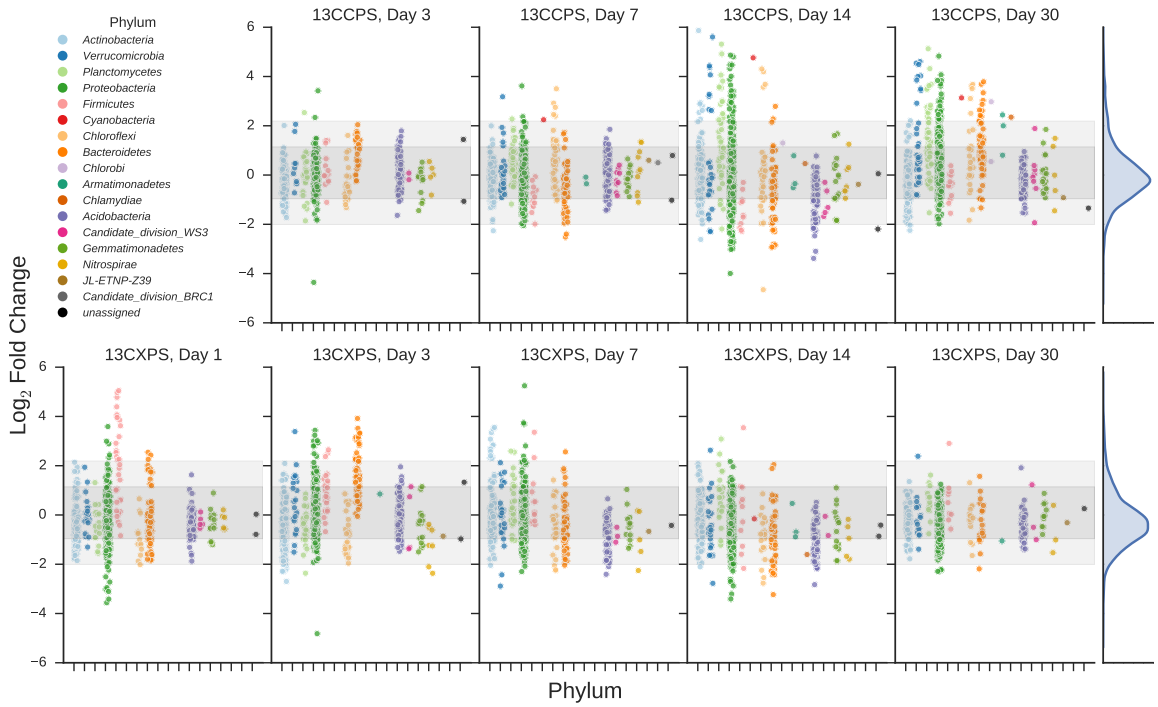

Fig. 2. OTU enrichment in ^{13}C-treatment heavy density fractions relative to control expressed as LFC (see Methods) for the ^{13}C-cellulose treatment (top) and ^{13}C-xylose treatment (bottom). High LFC indicate the OTU incorporated ^{13}C into DNA (each point represents an OTU LFC for the given treatment relative to control at the day indicated). Different colors represent different phyla and different panels represent different days. The final column shows the frequency distribution of LFC values in each row. Within each panel, shaded areas are used to indicate LFC plus or minus one standard deviation (dark shading) or two standard devations (light shading) about the mean of all LFC values.

bioRxiv preprint doi: https://doi.org/10.1101/022483; this version posted July 20, 2015. The copyright holder for this preprint (which was not certified by peer review) is the author/funder, who has granted bioRxiv a license to display the preprint in perpetuity. It is made available under a CC-BY-NC-ND 4.0 International license.

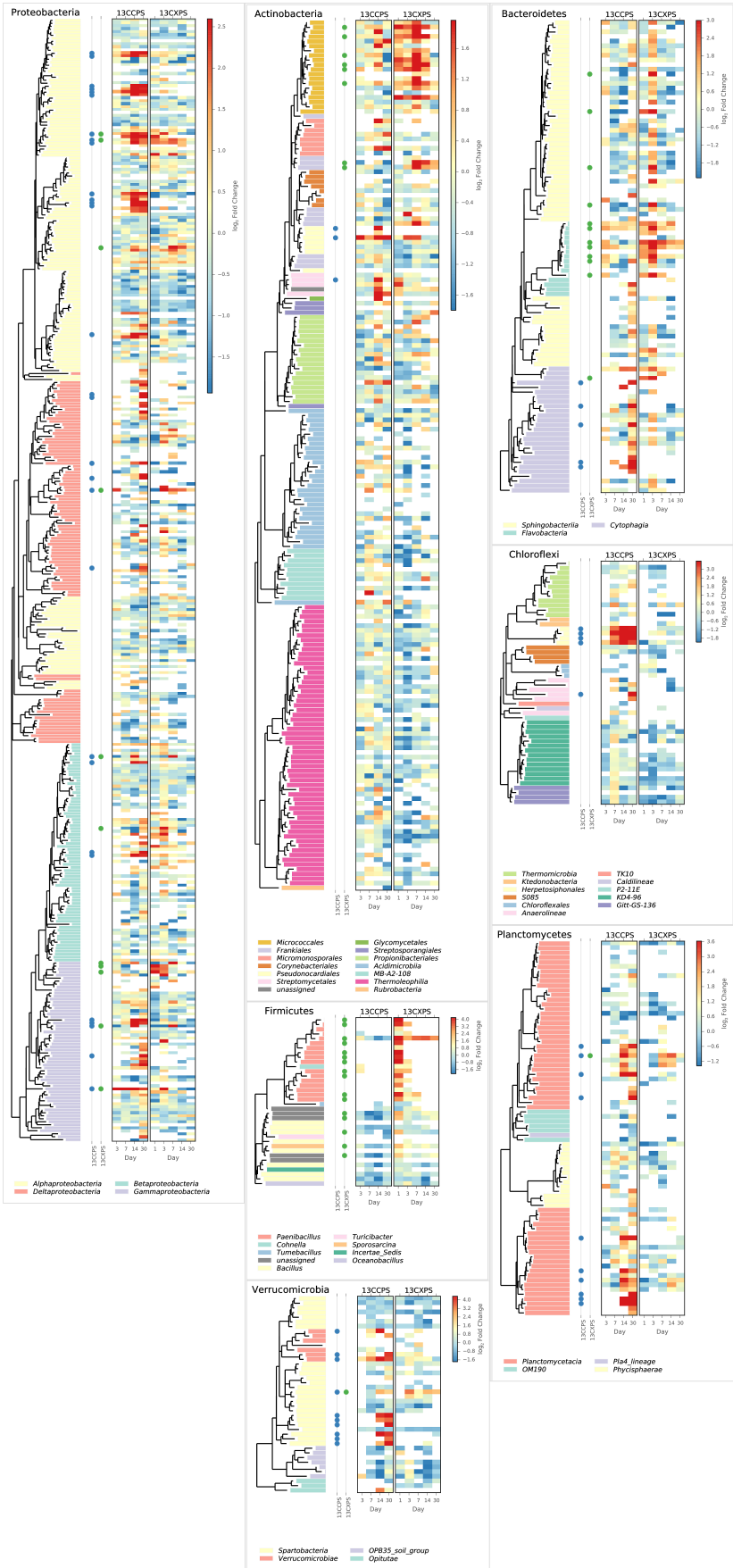

Fig. 3. Phylogenetic relationships of OTUs passing independent filtering when quantifying OTU enrichment in heavy gradient fractions relative to control (see Methods). Only those phyla that contain responders are shown. Colored dots are used to identify xylose responders (green) and cellulse responders (blue). The heatmaps indicate enrichment in high denstiy fractions relative to control (represented as LFC) for each OTU in response to both ^{13}C-cellulose ("13CCPS", leftmost heatmap) and ^{13}C-xylose ("13CXPS", rightmost heatmap) with values for different days in each heatmap column. Greater enrichment (represented as LFC) in heavy density fractions provide evidence of ^{13}C-labeled DNA.

bioRxiv preprint doi: https://doi.org/10.1101/022483; this version posted July 20, 2015. The copyright holder for this preprint (which was not certified by peer review) is the author/funder, who has granted bioRxiv a license to display the preprint in perpetuity. It is made available under a CC-BY-NC-ND 4.0 International license.

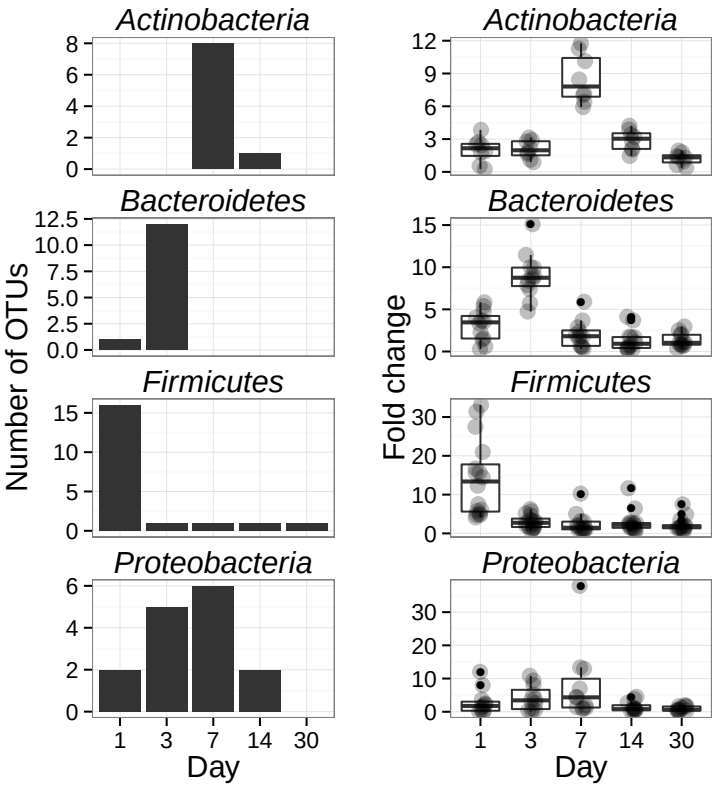

Fig. 4. Xylose reponders in the *Actinobacteria*, *Bacteroidetes*, *Firmicutes* exhibit distinct temporal dynamics of ^{13}C-labeling. The left column shows counts of ^{13}C-xylose responders in the *Actinobacteria*, *Bacteroidetes*, *Firmicutes* and *Proteobacteria* at days 1, 3, 7 and 30. The right panel shows enrichment in high density gradient fractions (expressed as fold change, not logarithmic) for responders (large points) as well as a boxplot for the distribution of fold change values (small dots are outliers, i.e. beyond 1.5 times the interquartile range (IR). Whiskers extend to 1.5 times the IR, and the box extends one IR about the median (solid line)). Each day in the right column shows all responders (i.e. OTUs that responded to xylose at any point in time). Greater enrichment in high density fractions of the ^{13}C-xylose treatment relative to control indicates DNA is ^{13}C-labeled.

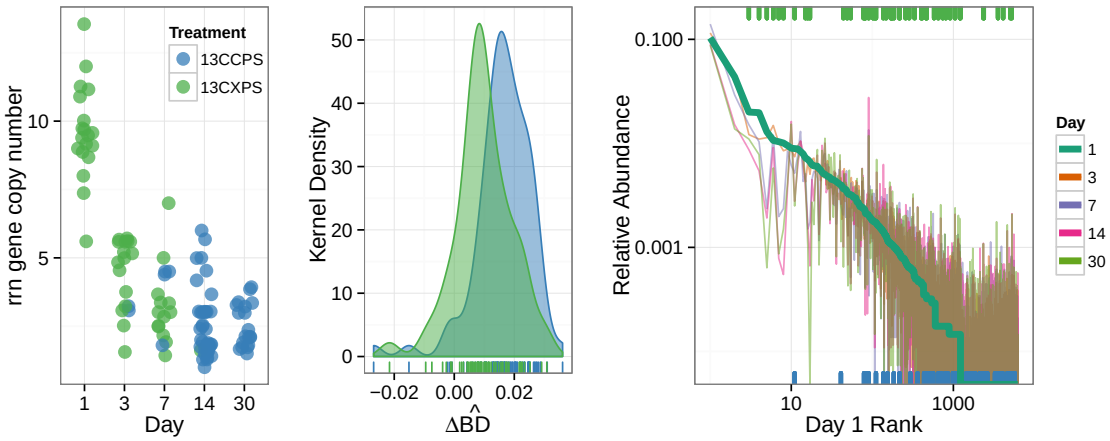

Fig. 5. Characteristics of xylose responders (green) and cellulose responders (blue) based on estimated *rrn* copy number (A), $\Delta\hat{BD}$ (B), and relative abundance in non-fractionated DNA (C). The estimated *rrn* copy number of all responders is shown versus time (A). Kernel density histogram of $\Delta\hat{BD}$ values shows cellulose responders had generally higher $\Delta\hat{BD}$ than xylose responders indicating potentially greater ^{13}C incorporation per unit DNA (B). The final panel indicates the rank relative abundance of all OTUs observed in the non-fractionated DNA (C) where rank was determined at day 1 (bold line) but relative abundance for each OTU is indicated for all days by colored lines (see legend). Xylose responders (green ticks) have higher relative abundance than xylose responders (ticks are based on day 1 relative abundance).

bioRxiv preprint doi: https://doi.org/10.1101/022483; this version posted July 20, 2015. The copyright holder for this preprint (which was not certified by peer review) is the author/funder, who has granted bioRxiv a license to display the preprint in perpetuity. It is made available under a CC-BY-NC-ND 4.0 International license.

Supplemental Figures and Tables

bioRxiv preprint doi: https://doi.org/10.1101/022483; this version posted July 20, 2015. The copyright holder for this preprint (which was not certified by peer review) is the author/funder, who has granted bioRxiv a license to display the preprint in perpetuity. It is made available under a CC-BY-NC-ND 4.0 International license.

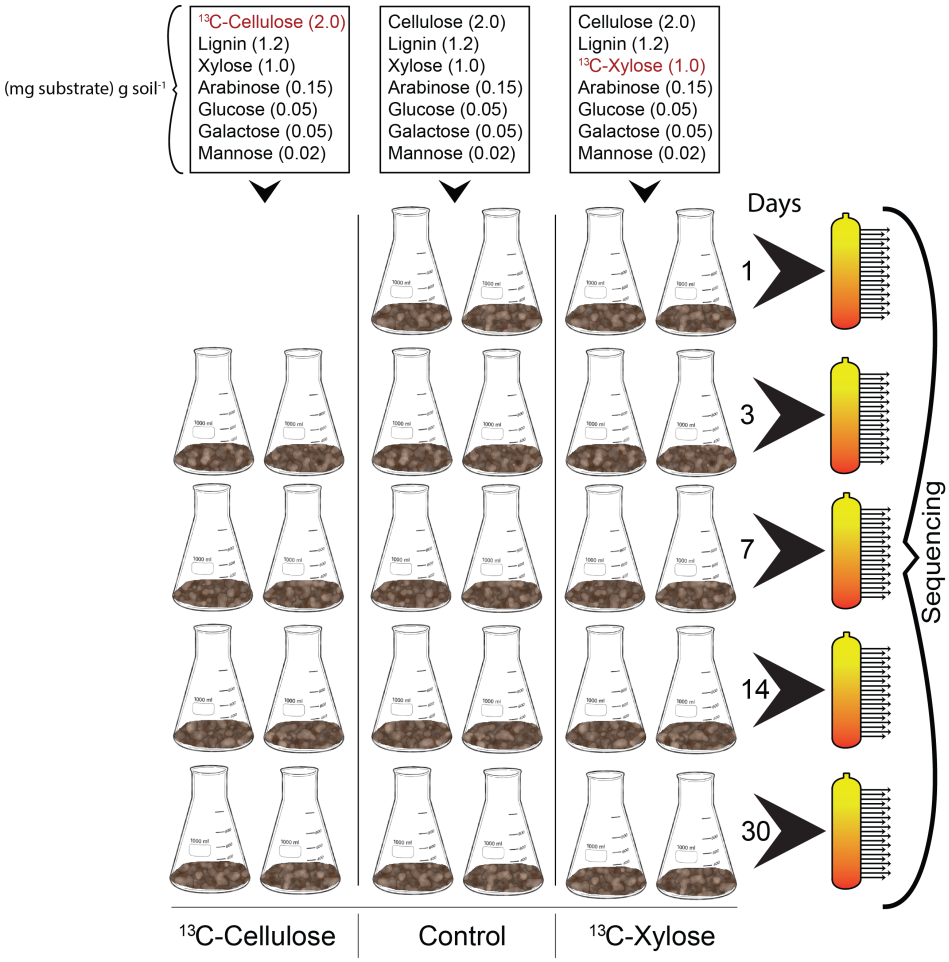

Fig. S1. An organic matter enrichment including C components and nutrients commonly found in plant biomass was added to soil microcosms. At days 1, 3, 7, 14, and 30 replicate microcosms were destructively harvested. Bulk DNA from each treatment and time point (n = 14) was subjected to CsCl density gradient centrifugation and density gradients were fractionated (orange tubes wherein each arrow represents a fraction from the density gradient). SSU rRNA genes were PCR amplified and sequenced from gradient fractions and from non-fractionated DNA (representing the bulk soil microbial community).

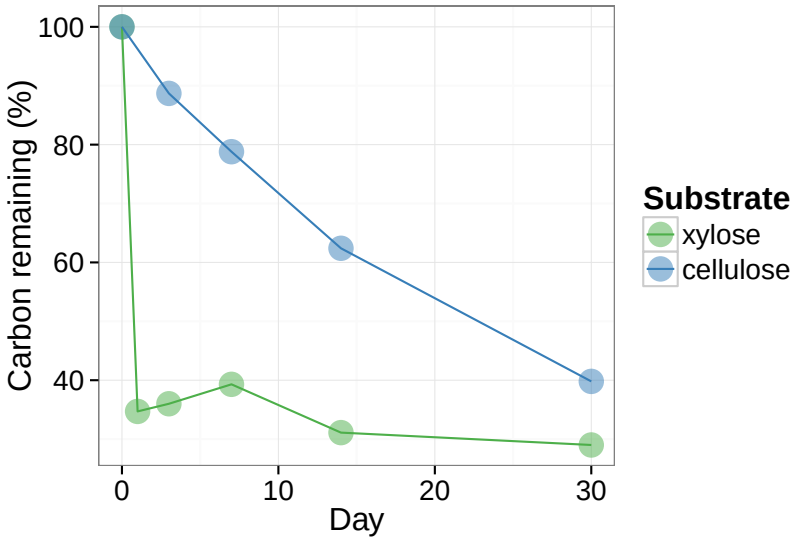

Fig. S2. Percentage of added ^{13}C remaining in soil over time.

bioRxiv preprint doi: https://doi.org/10.1101/022483; this version posted July 20, 2015. The copyright holder for this preprint (which was not certified by peer review) is the author/funder, who has granted bioRxiv a license to display the preprint in perpetuity. It is made available under a CC-BY-NC-ND 4.0 International license.

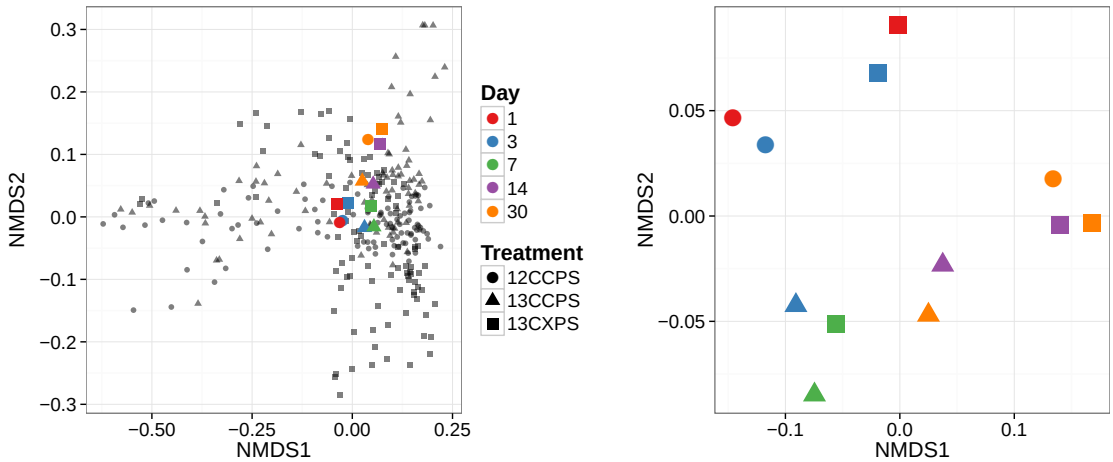

Fig. S3. NMDS analysis of SSU rRNA gene composition differences between non-fractionated DNA alone (right panel) and in the context of SIP gradient fractions (left panel). Non-fractionated DNA SSU rRNA gene composition changed with time but not with treatment (right panel) and variance of non-fractionated DNA SSU rRNA gene composition was less than variance introduced by density fractionation (left panel). Distance in SSU rRNA gene composition was quantified with the weighted UniFrac metric.

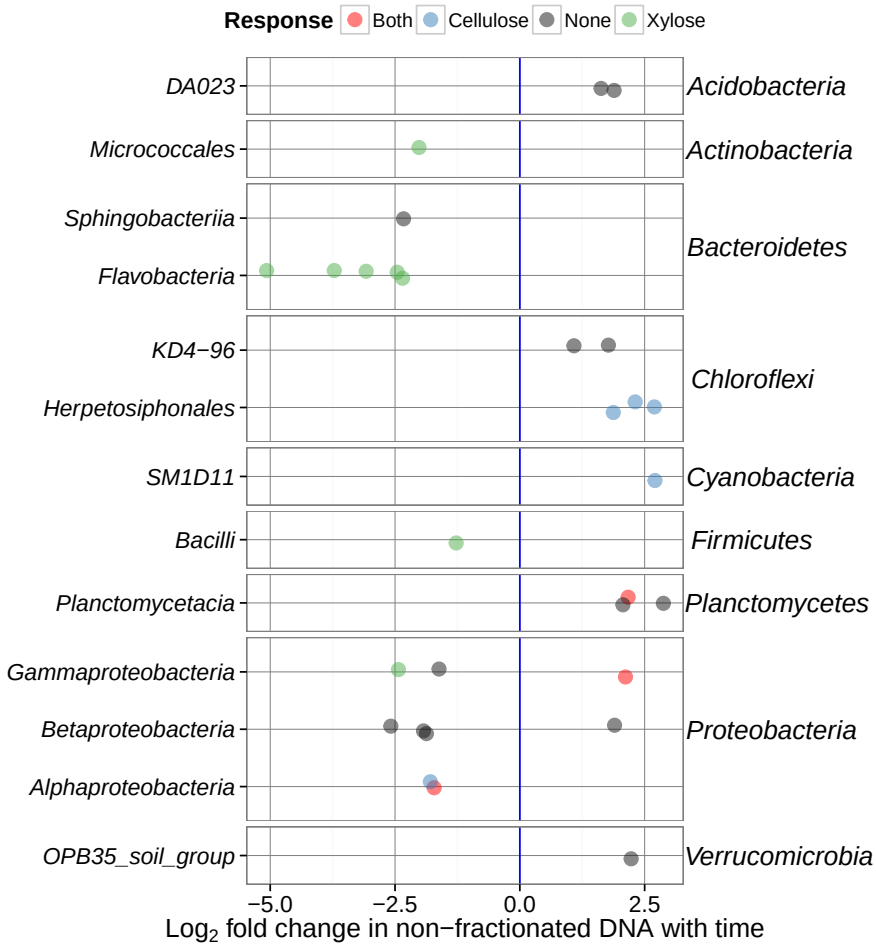

Fig. S4. Change in non-fractionated DNA relative abundance versus time (expressed as LFC) for OTUs that changed significantly (P-value < 0.10, Wald test). Each panel shows one phylum (labeled on the right). The taxonomic class is indicated on the left. Colors represent whether OTUs responded to just xylose (green), just cellulose (blue), or both xylose and cellulose (red).

bioRxiv preprint doi: https://doi.org/10.1101/022483; this version posted July 20, 2015. The copyright holder for this preprint (which was not certified by peer review) is the author/funder, who has granted bioRxiv a license to display the preprint in perpetuity. It is made available under a CC-BY-ND 4.0 International license.

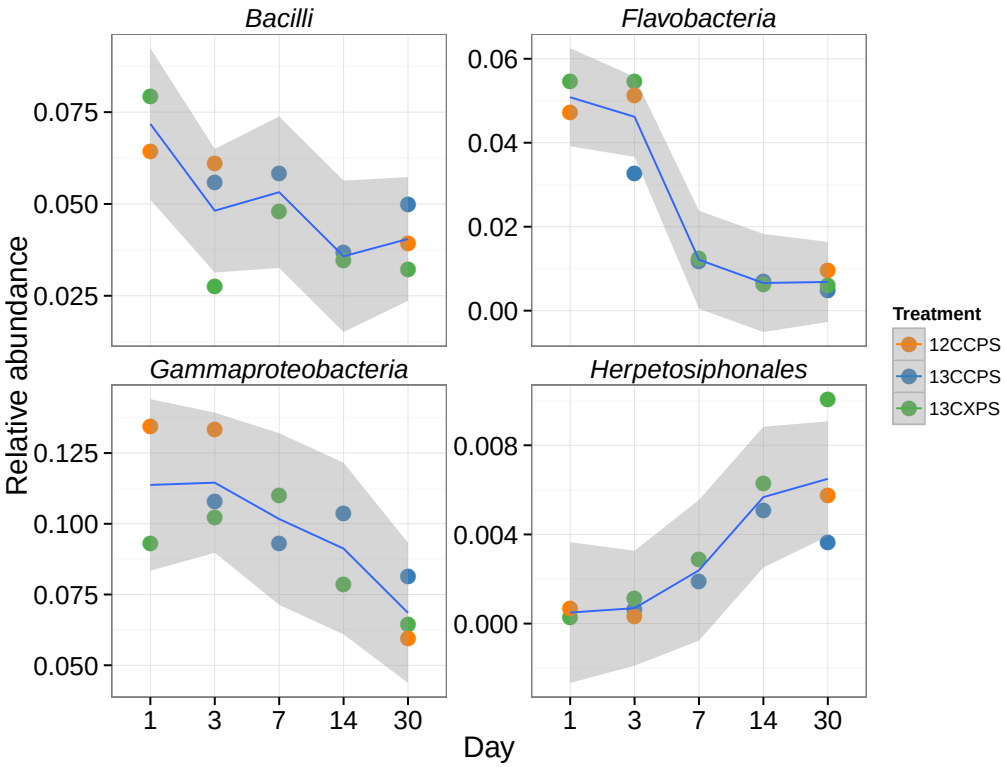

Fig. S5. Relative abundance in non-fractionated DNA versus time for classes that changed significantly.

bioRxiv preprint doi: https://doi.org/10.1101/022483; this version posted July 20, 2015. The copyright holder for this preprint (which was not certified by peer review) is the author/funder, who has granted bioRxiv a license to display the preprint in perpetuity. It is made available under a CC-BY-NC-ND 4.0 International license.

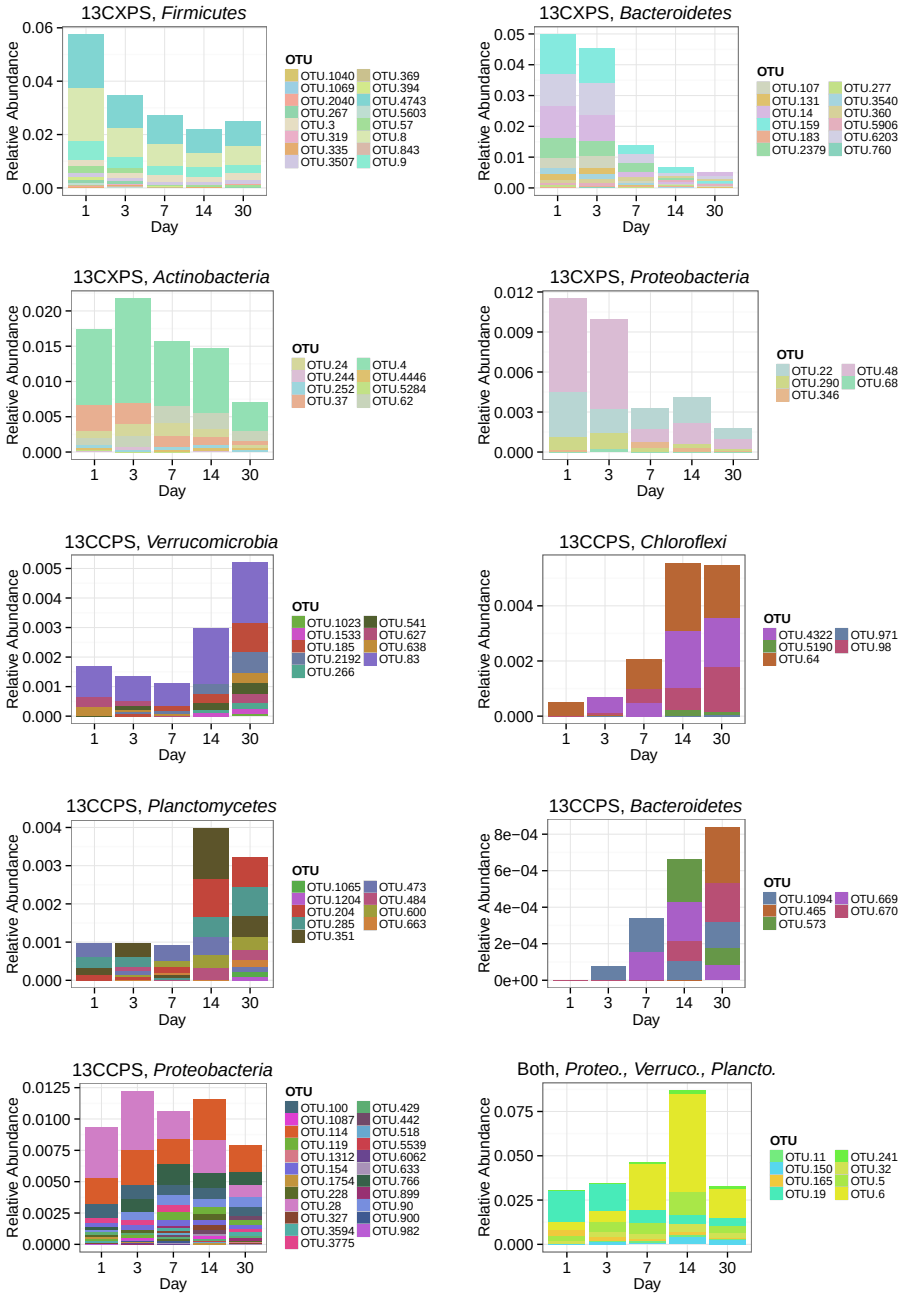

Fig. S6. Change in relative abundance in non-fractionated DNA over time for xylose responders (13CXPS) and cellulose responders (13CCPS). Each panel represents a phylum except for the lower right panel which shows all reponders to both xylose and celluose.

bioRxiv preprint doi: https://doi.org/10.1101/022483; this version posted July 20, 2015. The copyright holder for this preprint (which was not certified by peer review) is the author/funder, who has granted bioRxiv a license to display the preprint in perpetuity. It is made available under a CC-BY-ND 4.0 International license.

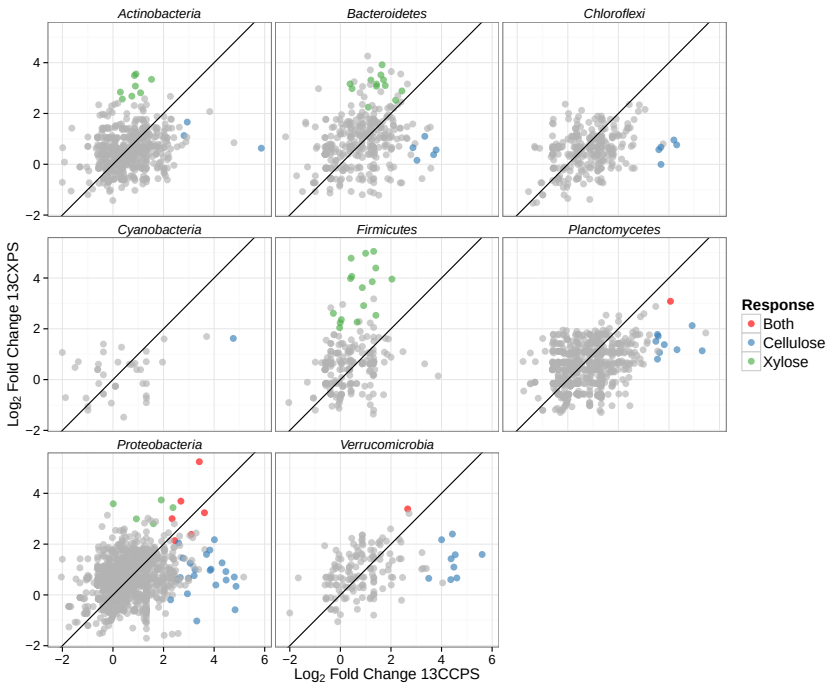

Fig. S7. Maximum enrichment at any point in time in heavy fractions of ^{13}C-treatments relative to control (expressed as LFC) shown for ^{13}C-cellulose versus ^{13}C-xylose treatments. Each point represents an OTU. Blue points are cellulose responders, green xylose responders, red are responders to both xylose and cellulose, and gray points are OTUs that did not repspond to either substrate. Line indicates a slope of one.

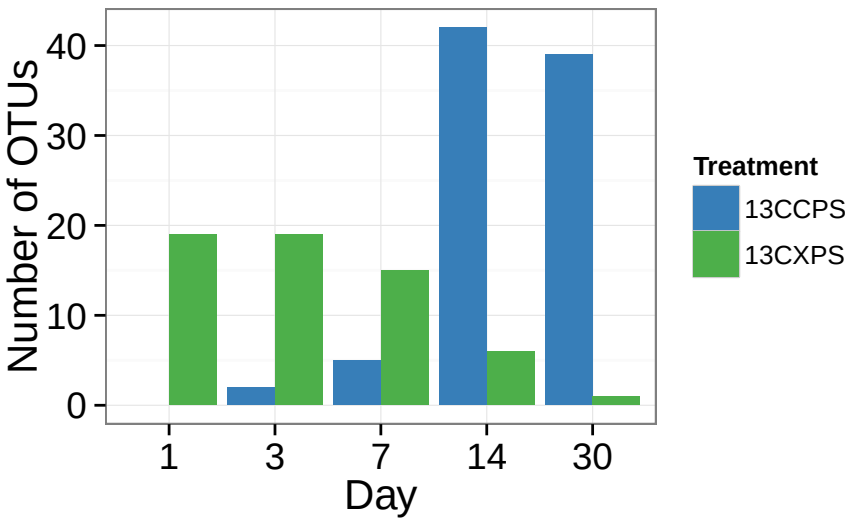

Fig. S8. Counts of xylose responders and cellulose responders over time.

bioRxiv preprint doi: https://doi.org/10.1101/022483; this version posted July 20, 2015. The copyright holder for this preprint (which was not certified by peer review) is the author/funder, who has granted bioRxiv a license to display the preprint in perpetuity. It is made available under a CC-BY-NC-ND 4.0 International license.

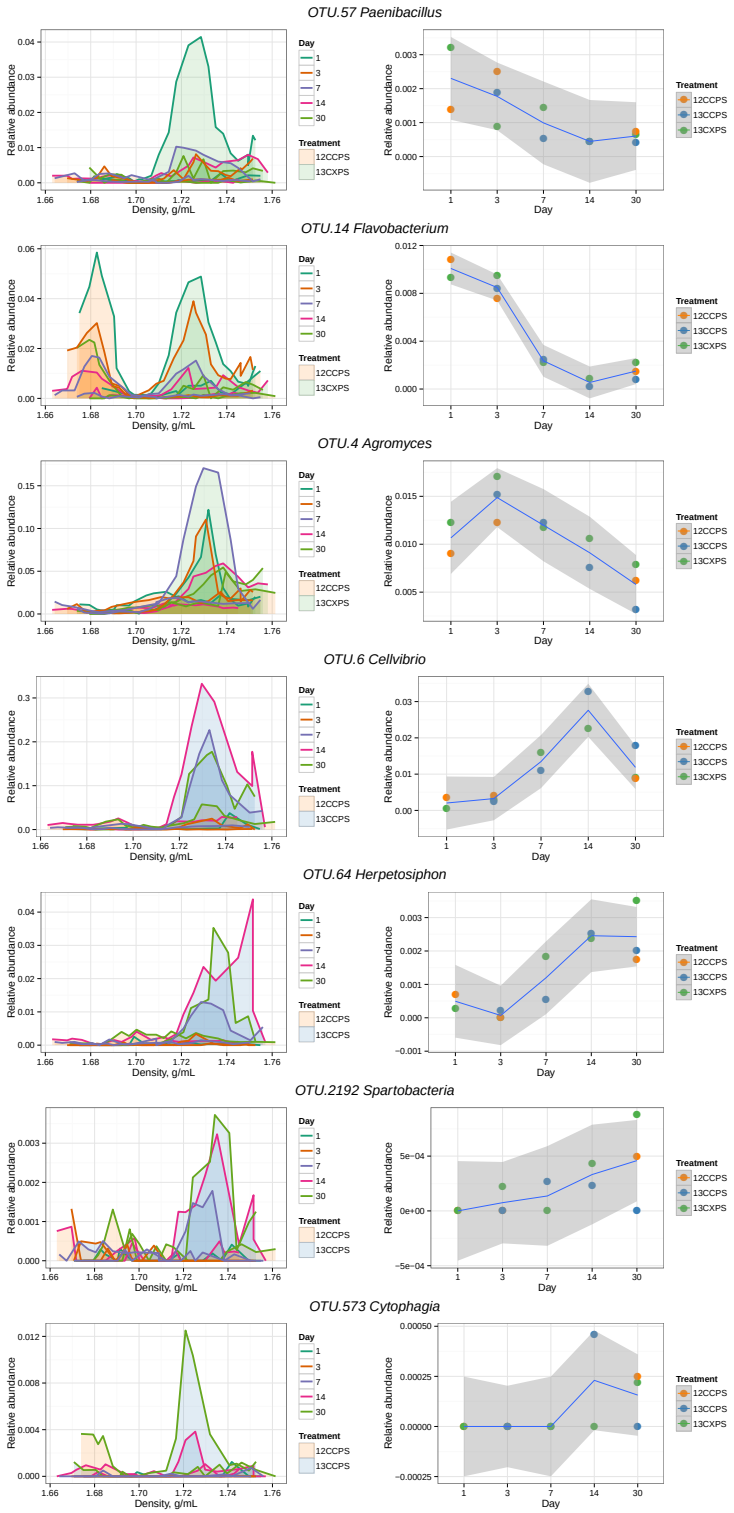

Fig. S9. Raw data from example responders highlighted in the main text (see Results). The left column shows DNA-SIP density fraction relative abundances for ^{13}C-xylose or ^{13}C-cellulose gradients in addition to control gradients for each of the chosen OTUs. Time is indicated by the color of the relative abundance profile (see legend). Gradient profiles are shaded by treatment where orange represents "control" profles, blue "^{13}C-cellulose", and green "^{13}C-xylose." The right column shows the relative abundance of each OTU in non-fractionated DNA (i.e. the DNA that was subsequently fractionated on the density gradient). Enrichment in the heavy end of the gradient in ^{13}C-treatments indicates an OTU has ^{13}C-labeled DNA.

bioRxiv preprint doi: https://doi.org/10.1101/022483; this version posted July 20, 2015. The copyright holder for this preprint (which was not certified by peer review) is the author/funder, who has granted bioRxiv a license to display the preprint in perpetuity. It is made available under a CC-BY-NC-ND 4.0 International license.

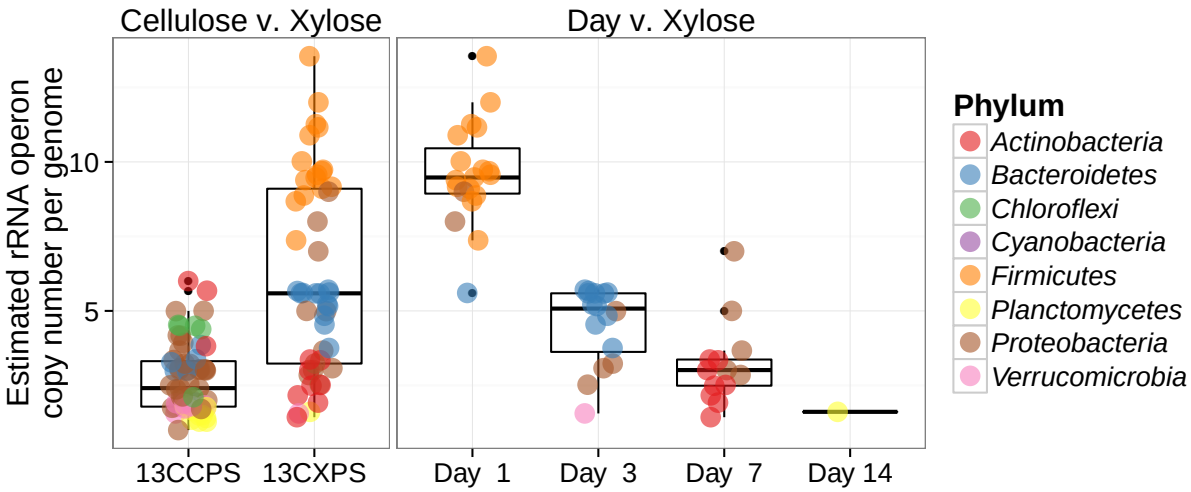

Fig. S10. Estimated rrn copy number for xylose and cellulose responders. The leftmost panel contrasts estimated rrn copy number for cellulose (13CCPS) and xylose (13CXPS) responders. The right panel shows estimated rrn copy number versus time of first response for xylose responders. Colors denote the phylum of the OTUs (see legend).

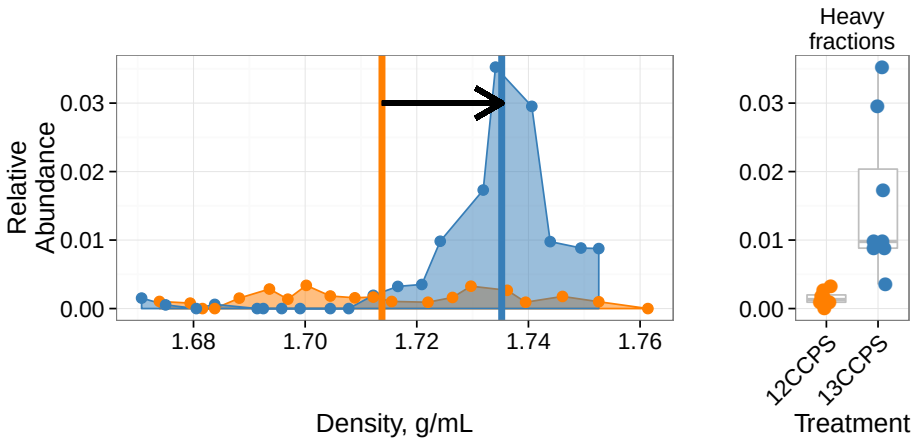

Fig. S11. Density profile for a single cellulose responder in the ^{13}C-cellulose treatment (blue) and control (orange). Vertical lines show center of mass for each density profile and the arrow denotes the magnitude and direction of $\Delta\hat{BD}$. Right panel shows relative abundance values in the high density fractions (The boxplot line is the median value. The box spans one interquartile range (IR) about the median, whiskers extend 1.5 times the IR and the dots indicate outlier values beyond 1.5 times the IR).

bioRxiv preprint doi: https://doi.org/10.1101/022483; this version posted July 20, 2015. The copyright holder for this preprint (which was not certified by peer review) is the author/funder, who has granted bioRxiv a license to display the preprint in perpetuity. It is made available under a CC-BY-NC-ND 4.0 International license.

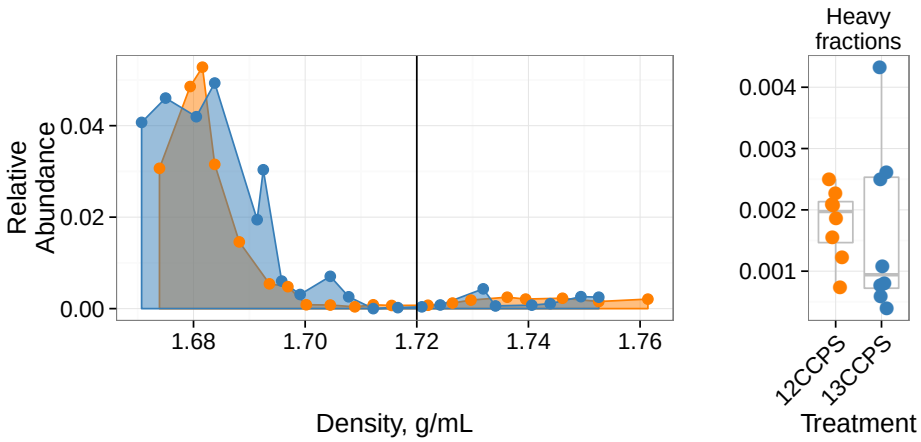

Fig. S12. Density profile for a single non-responder OTU. The ^{13}C-cellulose treatment is in blue and the control treatment is in orange. The vertical line shows where "heavy" fractions begin as defined in our analysis. The right panel shows relative abundance values in the heavy fractions for each gradient (The boxplot line is the median value. The box spans one interquartile range (IR) about the median, whiskers extend 1.5 times the IR and the dots indicate outlier values beyond 1.5 times the IR).

bioRxiv preprint doi: https://doi.org/10.1101/022483; this version posted July 20, 2015. The copyright holder for this preprint (which was not certified by peer review) is the author/funder, who has granted bioRxiv a license to display the preprint in perpetuity. It is made available under a CC-BY-NC-ND 4.0 International license.

Table S1: ^{13}C-xylose responders BLAST against Living Tree Project

OTU ID	Fold change [a]	Day [b]	All days [c]	Top BLAST hits	BLAST %ID	Phylum;Class;Order
OTU.1040	4.78	1	1	*Paenibacillus daejeonensis*	100.0	*Firmicutes Bacilli Bacillales*
OTU.1069	3.85	1	1	*Paenibacillus terrigena*	100.0	*Firmicutes Bacilli Bacillales*
OTU.107	2.25	3	3	*Flavobacterium sp. 15C3*, *Flavobacterium banpakuense*	99.54	*Bacteroidetes Flavobacteria Flavobacteriales*
OTU.11	5.25	7	7	*Stenotrophomonas pavanii*, *Stenotrophomonas maltophilia*, *Pseudomonas geniculata*	99.54	*Proteobacteria Gammaproteobacteria Xanthomonadales*
OTU.131	3.07	3	3	*Flavobacterium fluvii*, *Flavobacteria bacterium HMD1033*, *Flavobacterium sp. HMD1001*	100.0	*Bacteroidetes Flavobacteria Flavobacteriales*
OTU.14	3.92	3	1, 3	*Flavobacterium oncorhynchi*, *Flavobacterium glycines*, *Flavobacterium succinicans*	99.09	*Bacteroidetes Flavobacteria Flavobacteriales*
OTU.150	3.08	14	14	No hits of at least 90% identity	86.76	*Planctomycetes Planctomycetacia Planctomycetales*
OTU.159	3.16	3	3	*Flavobacterium hibernum*	98.17	*Bacteroidetes Flavobacteria Flavobacteriales*
OTU.165	2.38	3	3	*Rhizobium skierniewicense*, *Rhizobium vignae*, *Rhizobium larrymoorei*, *Rhizobium alkalisoli*, *Rhizobium galegae*, *Rhizobium huautlense*	100.0	*Proteobacteria Alphaproteobacteria Rhizobiales*
OTU.183	3.31	3	3	No hits of at least 90% identity	89.5	*Bacteroidetes Sphingobacteriia Sphingobacteriales*
OTU.19	2.14	7	7	*Rhizobium alamii*, *Rhizobium mesosinicum*, *Rhizobium mongolense*, *Arthrobacter viscosus*, *Rhizobium sullae*, *Rhizobium yanglingense*, *Rhizobium loessense*	99.54	*Proteobacteria Alphaproteobacteria Rhizobiales*
OTU.2040	2.91	1	1	*Paenibacillus pectinilyticus*	100.0	*Firmicutes Bacilli Bacillales*
OTU.22	2.8	7	7, 14	*Paracoccus sp. NB88*	99.09	*Proteobacteria Alphaproteobacteria Rhodobacterales*
OTU.2379	3.1	3	3	*Flavobacterium pectinovorum*, *Flavobacterium sp. CS100*	97.72	*Bacteroidetes Flavobacteria Flavobacteriales*
OTU.24	2.81	7	7	*Cellulomonas aerilata*, *Cellulomonas humilata*, *Cellulomonas terrae*, *Cellulomonas soli*, *Cellulomonas xylanilytica*	100.0	*Actinobacteria Micrococcales Cellulomonadaceae*
OTU.241	3.38	3	3, 14	No hits of at least 90% identity	87.73	*Verrucomicrobia Spartobacteria Chthoniobacterales*
OTU.244	3.08	7	7	*Cellulosimicrobium funkei*, *Cellulosimicrobium terreum*	100.0	*Actinobacteria Micrococcales Promicromonosporaceae*
OTU.252	3.34	7	7	*Promicromonospora thailandica*	100.0	*Actinobacteria Micrococcales Promicromonosporaceae*
OTU.267	4.97	1	1	*Paenibacillus pabuli*, *Paenibacillus tundrae*, *Paenibacillus taichungensis*, *Paenibacillus xylanexedens*, *Paenibacillus xylanilyticus*	100.0	*Firmicutes Bacilli Bacillales*
OTU.277	3.52	3	3	*Solibius ginsengiterrae*	95.43	*Bacteroidetes Sphingobacteriia Sphingobacteriales*

bioRxiv preprint doi: https://doi.org/10.1101/022483; this version posted July 20, 2015. The copyright holder for this preprint (which was not certified by peer review) is the author/funder, who has granted bioRxiv a license to display the preprint in perpetuity. It is made available under a CC-BY-NC-ND 4.0 International license.

Table S1 – continued from previous page

OTU ID	Fold change	Day	All days	Top BLAST hits	BLAST %ID	Phylum;Class;Order
OTU.290	3.59	1	1	*Pantoea spp.*, *Kluyvera spp.*, *Klebsiella spp.*, *Erwinia spp.*, *Enterobacter spp.*, *Buttiauxella spp.*	100.0	*Proteobacteria Gammaproteobacteria Enterobacteriales*
OTU.3	2.61	1	1	*[Brevibacterium] frigoritolerans*, *Bacillus sp. LMG 20238*, *Bacillus coahuilensis m4-4*, *Bacillus simplex*	100.0	*Firmicutes Bacilli Bacillales*
OTU.319	3.98	1	1	*Paenibacillus xinjiangensis*	97.25	*Firmicutes Bacilli Bacillales*
OTU.32	3.0	3	3, 7, 14	*Sandaracinus amylolyticus*	94.98	*Proteobacteria Deltaproteobacteria Myxococcales*
OTU.335	2.53	1	1	*Paenibacillus thailandensis*	98.17	*Firmicutes Bacilli Bacillales*
OTU.346	3.44	3	3	*Pseudoduganella violaceinigra*	99.54	*Proteobacteria Betaproteobacteria Burkholderiales*
OTU.3507	2.36	1	1	*Bacillus spp.*	98.63	*Firmicutes Bacilli Bacillales*
OTU.3540	2.52	3	3	*Flavobacterium terrigena*	99.54	*Bacteroidetes Flavobacteria Flavobacteriales*
OTU.360	2.98	3	3	*Flavisolibacter ginsengisoli*	95.0	*Bacteroidetes Sphingobacteriia Sphingobacteriales*
OTU.369	5.05	1	1	*Paenibacillus sp. D75*, *Paenibacillus glycanilyticus*	100.0	*Firmicutes Bacilli Bacillales*
OTU.37	2.68	7	7	*Phycicola gilvus*, *Microterricola viridarii*, *Frigoribacterium faeni*, *Frondihabitans sp. RS-15*, *Frondihabitans australicus*	100.0	*Actinobacteria Micrococcales Microbacteriaceae*
OTU.394	4.06	1	1	*Paenibacillus pocheonensis*	100.0	*Firmicutes Bacilli Bacillales*
OTU.4	2.84	7	7, 14	*Agromyces ramosus*	100.0	*Actinobacteria Micrococcales Microbacteriaceae*
OTU.4446	3.49	7	7	*Catenuloplanes niger*, *Catenuloplanes castaneus*, *Catenuloplanes atrovinosus*, *Catenuloplanes crispus*, *Catenuloplanes nepalensis*, *Catenuloplanes japonicus*	97.72	*Actinobacteria Frankiales Nakamurellaceae*
OTU.4743	2.24	1	1	*Lysinibacillus fusiformis*, *Lysinibacillus sphaericus*	99.09	*Firmicutes Bacilli Bacillales*
OTU.48	2.99	1	1, 3	*Aeromonas spp.*	100.0	*Proteobacteria Gammaproteobacteria aaa34a10*
OTU.5	3.69	7	7	*Delftia tsuruhatensis*, *Delftia lacustris*	100.0	*Proteobacteria Betaproteobacteria Burkholderiales*
OTU.5284	3.56	7	7	*Isoptericola nanjingensis*, *Isoptericola hypogeus*, *Isoptericola variabilis*	98.63	*Actinobacteria Micrococcales Promicromonosporaceae*
OTU.5603	3.96	1	1	*Paenibacillus uliginis*	100.0	*Firmicutes Bacilli Bacillales*
OTU.57	4.39	1	1, 3, 7, 14, 30	*Paenibacillus castaneae*	98.62	*Firmicutes Bacilli Bacillales*
OTU.5906	3.16	3	3	*Terrimonas sp. M-8*	96.8	*Bacteroidetes Sphingobacteriia Sphingobacteriales*
OTU.6	3.24	3	3	*Cellvibrio fulvus*	100.0	*Proteobacteria Gammaproteobacteria Pseudomonadales*

bioRxiv preprint doi: https://doi.org/10.1101/022483; this version posted July 20, 2015. The copyright holder for this preprint (which was not certified by peer review) is the author/funder, who has granted bioRxiv a license to display the preprint in perpetuity. It is made available under a CC-BY-ND 4.0 International license.

Table S1 – continued from previous page

OTU ID	Fold change	Day	All days	Top BLAST hits	BLAST %ID	Phylum;Class;Order
OTU.62	2.57	7	7	*Nakamurella flavida*	100.0	*Actinobacteria Frankiales Nakamurellaceae*
OTU.6203	3.32	3	3	*Flavobacterium granuli*, *Flavobacterium glaciei*	100.0	*Bacteroidetes Flavobacteria Flavobacteriales*
OTU.68	3.74	7	7	*Shigella flexneri*, *Escherichia fergusonii*, *Escherichia coli*, *Shigella sonnei*	100.0	*Proteobacteria Gammaproteobacteria Enterobacteriales*
OTU.760	2.89	3	3	*Dyadobacter hamtensis*	98.63	*Bacteroidetes Cytophagia Cytophagales*
OTU.8	2.26	1	1	*Bacillus niacini*	100.0	*Firmicutes Bacilli Bacillales*
OTU.843	3.62	1	1	*Paenibacillus agarexedens*	100.0	*Firmicutes Bacilli Bacillales*
OTU.9	2.04	1	1	*Bacillus megaterium*, *Bacillus flexus*	100.0	*Firmicutes Bacilli Bacillales*

[a] Maximum observed log_2 of fold change.
[b] Day of maximum fold change.
[c] All response days.

bioRxiv preprint doi: https://doi.org/10.1101/022483; this version posted July 20, 2015. The copyright holder for this preprint (which was not certified by peer review) is the author/funder, who has granted bioRxiv a license to display the preprint in perpetuity. It is made available under a CC-BY-NC-ND 4.0 International license.

Table S2: ^{13}C-cellulose responders BLAST against Living Tree Project

OTU ID	Fold change [a]	Day [b]	All days [c]	Top BLAST hits	BLAST %ID	Phylum;Class;Order
OTU.100	2.66	14	14	*Pseudoxanthomonas sacheonensis*, *Pseudoxanthomonas dokdonensis*	100.0	*Proteobacteria Gammaproteobacteria Xanthomonadales*
OTU.1023	4.61	30	30	No hits of at least 90% identity	80.54	*Verrucomicrobia Spartobacteria Chthoniobacterales*
OTU.1065	5.31	14	14, 30	No hits of at least 90% identity	84.55	*Planctomycetes Planctomycetacia Planctomycetales*
OTU.1087	4.32	14	14, 30	*Devosia soli*, *Devosia crocina*, *Devosia riboflavina*	99.09	*Proteobacteria Alphaproteobacteria Rhizobiales*
OTU.1094	3.69	30	30	*Sporocytophaga myxococcoides*	99.55	*Bacteroidetes Cytophagia Cytophagales*
OTU.11	3.41	14	14	*Stenotrophomonas pavanii*, *Stenotrophomonas maltophilia*, *Pseudomonas geniculata*	99.54	*Proteobacteria Gammaproteobacteria Xanthomonadales*
OTU.114	2.78	14	14	*Herbaspirillum sp. SUEMI03*, *Herbaspirillum sp. SUEMI10*, *Oxalicibacterium solurbis*, *Herminiimonas fonticola*, *Oxalicibacterium horti*	100.0	*Proteobacteria Betaproteobacteria Burkholderiales*
OTU.119	3.31	14	14, 30	*Brevundimonas alba*	100.0	*Proteobacteria Alphaproteobacteria Caulobacterales*
OTU.120	4.76	14	14, 30	*Vampirovibrio chlorellavorus*	94.52	*Cyanobacteria SM1D11 uncultured-bacterium*
OTU.1204	4.32	30	30	*Planctomyces limnophilus*	91.78	*Planctomycetes Planctomycetacia Planctomycetales*
OTU.1312	4.07	30	30	*Paucimonas lemoignei*	99.54	*Proteobacteria Betaproteobacteria Burkholderiales*
OTU.132	2.81	14	14	*Streptomyces spp.*	100.0	*Actinobacteria Streptomycetales Streptomycetaceae*
OTU.150	4.06	14	14	No hits of at least 90% identity	86.76	*Planctomycetes Planctomycetacia Planctomycetales*
OTU.1533	3.43	30	30	No hits of at least 90% identity	82.27	*Verrucomicrobia Spartobacteria Chthoniobacterales*
OTU.154	3.24	14	14	*Pseudoxanthomonas mexicana*, *Pseudoxanthomonas japonensis*	100.0	*Proteobacteria Gammaproteobacteria Xanthomonadales*
OTU.165	3.1	14	14	*Rhizobium skierniewicense*, *Rhizobium vignae*, *Rhizobium larrymoorei*, *Rhizobium alkalisoli*, *Rhizobium galegae*, *Rhizobium huautlense*	100.0	*Proteobacteria Alphaproteobacteria Rhizobiales*
OTU.1754	4.48	14	14	*Asticcacaulis biprosthecium*, *Asticcacaulis benevestitus*	96.8	*Proteobacteria Alphaproteobacteria Caulobacterales*
OTU.185	4.37	14	14, 30	No hits of at least 90% identity	85.14	*Verrucomicrobia Spartobacteria Chthoniobacterales*
OTU.19	2.44	14	14	*Rhizobium alamii*, *Rhizobium mesosinicum*, *Rhizobium mongolense*, *Arthrobacter viscosus*, *Rhizobium sullae*, *Rhizobium yanglingense*, *Rhizobium loessense*	99.54	*Proteobacteria Alphaproteobacteria Rhizobiales*

bioRxiv preprint doi: https://doi.org/10.1101/022483; this version posted July 20, 2015. The copyright holder for this preprint (which was not certified by peer review) is the author/funder, who has granted bioRxiv a license to display the preprint in perpetuity. It is made available under a CC-BY-ND 4.0 International license.

Table S2 – continued from previous page

OTU ID	Fold change	Day	All days	Top BLAST hits	BLAST %ID	Phylum;Class;Order
OTU.2192	3.49	30	14, 30	No hits of at least 90% identity	83.56	*Verrucomicrobia Spartobacteria Chthoniobacterales*
OTU.228	2.54	30	30	*Sorangium cellulosum*	98.17	*Proteobacteria Deltaproteobacteria Myxococcales*
OTU.241	2.66	14	14	No hits of at least 90% identity	87.73	*Verrucomicrobia Spartobacteria Chthoniobacterales*
OTU.257	2.94	14	14	*Lentzea waywayandensis*, *Lentzea flaviverrucosa*	100.0	*Actinobacteria Pseudonocardiales Pseudonocardiaceae*
OTU.266	4.54	30	14, 30	No hits of at least 90% identity	83.64	*Verrucomicrobia Spartobacteria Chthoniobacterales*
OTU.28	2.59	14	14	*Rhizobium giardinii*, *Rhizobium tubonense*, *Rhizobium tibeticum*, *Rhizobium mesoamericanum CCGE 501*, *Rhizobium herbae*, *Rhizobium endophyticum*	99.54	*Proteobacteria Alphaproteobacteria Rhizobiales*
OTU.285	3.55	30	14, 30	*Blastopirellula marina*	90.87	*Planctomycetes Planctomycetacia Planctomycetales*
OTU.32	2.34	3	3	*Sandaracinus amylolyticus*	94.98	*Proteobacteria Deltaproteobacteria Myxococcales*
OTU.327	2.99	14	14	*Asticcacaulis biprosthecium*, *Asticcacaulis benevestitus*	98.63	*Proteobacteria Alphaproteobacteria Caulobacterales*
OTU.351	3.54	14	14, 30	*Pirellula staleyi DSM 6068*	91.86	*Planctomycetes Planctomycetacia Planctomycetales*
OTU.3594	3.83	30	30	*Chondromyces robustus*	90.41	*Proteobacteria Deltaproteobacteria Myxococcales*
OTU.3775	3.88	14	14	*Devosia glacialis*, *Devosia chinhatensis*, *Devosia geojensis*, *Devosia yakushimensis*	98.63	*Proteobacteria Alphaproteobacteria Rhizobiales*
OTU.429	3.7	30	14, 30	*Devosia limi*, *Devosia psychrophila*	97.72	*Proteobacteria Alphaproteobacteria Rhizobiales*
OTU.4322	4.19	14	7, 14, 30	No hits of at least 90% identity	89.14	*Chloroflexi Herpetosiphonales Herpetosiphonaceae*
OTU.442	3.05	30	30	*Chondromyces robustus*	92.24	*Proteobacteria Deltaproteobacteria Myxococcales*
OTU.465	3.79	30	30	*Ohtaekwangia kribbensis*	92.73	*Bacteroidetes Cytophagia Cytophagales*
OTU.473	3.58	14	14	*Pirellula staleyi DSM 6068*	90.91	*Planctomycetes Planctomycetacia Planctomycetales*
OTU.484	4.92	14	14, 30	No hits of at least 90% identity	89.09	*Planctomycetes Planctomycetacia Planctomycetales*
OTU.5	2.69	14	14	*Delftia tsuruhatensis*, *Delftia lacustris*	100.0	*Proteobacteria Betaproteobacteria Burkholderiales*
OTU.518	4.8	14	14	*Hydrogenophaga intermedia*	100.0	*Proteobacteria Betaproteobacteria Burkholderiales*
OTU.5190	3.6	30	14, 30	No hits of at least 90% identity	88.13	*Chloroflexi Herpetosiphonales Herpetosiphonaceae*
OTU.541	4.49	30	30	No hits of at least 90% identity	84.23	*Verrucomicrobia Spartobacteria Chthoniobacterales*
OTU.5539	4.01	14	14	*Devosia subaequoris*	98.17	*Proteobacteria Alphaproteobacteria Rhizobiales*
OTU.573	3.03	30	30	*Adhaeribacter aerophilus*	92.76	*Bacteroidetes Cytophagia Cytophagales*

bioRxiv preprint doi: https://doi.org/10.1101/022483; this version posted July 20, 2015. The copyright holder for this preprint (which was not certified by peer review) is the author/funder, who has granted bioRxiv a license to display the preprint in perpetuity. It is made available under a CC-BY-ND 4.0 International license.

Table S2 – continued from previous page

OTU ID	Fold change	Day	All days	Top BLAST hits	BLAST %ID	Phylum;Class;Order
OTU.6	3.62	7	3, 7, 14	*Cellvibrio fulvus*	100.0	*Proteobacteria Gammaproteobacteria Pseudomonadales*
OTU.600	3.48	30	30	No hits of at least 90% identity	80.37	*Planctomycetes Planctomycetacia Planctomycetales*
OTU.6062	4.83	30	30	*Dokdonella sp. DC-3*, *Luteibacter rhizovicinus*	97.26	*Proteobacteria Gammaproteobacteria Xanthomonadales*
OTU.627	4.43	14	14	*Verrucomicrobiaceae bacterium DC2a-G7*	100.0	*Verrucomicrobia Verrucomicrobiae Verrucomicrobiales*
OTU.633	3.84	30	30	No hits of at least 90% identity	89.5	*Proteobacteria Deltaproteobacteria Myxococcales*
OTU.638	4.0	30	30	*Luteolibacter sp. CCTCC AB 2010415*, *Luteolibacter algae*	93.61	*Verrucomicrobia Verrucomicrobiae Verrucomicrobiales*
OTU.64	4.31	14	7, 14, 30	No hits of at least 90% identity	89.5	*Chloroflexi Herpetosiphonales Herpetosiphonaceae*
OTU.663	3.63	30	30	*Pirellula staleyi DSM 6068*	90.87	*Planctomycetes Planctomycetacia Planctomycetales*
OTU.669	3.34	30	30	*Ohtaekwangia koreensis*	92.69	*Bacteroidetes Cytophagia Cytophagales*
OTU.670	2.87	30	30	*Adhaeribacter aerophilus*	91.78	*Bacteroidetes Cytophagia Cytophagales*
OTU.766	3.21	14	14, 30	*Devosia insulae*	99.54	*Proteobacteria Alphaproteobacteria Rhizobiales*
OTU.83	5.61	14	7, 14, 30	*Luteolibacter sp. CCTCC AB 2010415*	97.72	*Verrucomicrobia Verrucomicrobiae Verrucomicrobiales*
OTU.862	5.87	14	14	*Allokutzneria albata*	100.0	*Actinobacteria Pseudonocardiales Pseudonocardiaceae*
OTU.899	2.28	30	30	*Enhygromyxa salina*	97.72	*Proteobacteria Deltaproteobacteria Myxococcales*
OTU.90	2.94	14	14, 30	*Sphingopyxis panaciterrae*, *Sphingopyxis chilensis*, *Sphingopyxis sp. BZ30*, *Sphingomonas sp.*	100.0	*Proteobacteria Alphaproteobacteria Sphingomonadales*
OTU.900	4.87	14	14	*Brevundimonas vesicularis*, *Brevundimonas nasdae*	100.0	*Proteobacteria Alphaproteobacteria Caulobacterales*
OTU.971	3.68	30	30	No hits of at least 90% identity	78.57	*Chloroflexi Anaerolineae Anaerolineales*
OTU.98	3.68	14	7, 14, 30	No hits of at least 90% identity	88.18	*Chloroflexi Herpetosiphonales Herpetosiphonaceae*
OTU.982	4.47	14	14	*Devosia neptuniae*	100.0	*Proteobacteria Alphaproteobacteria Rhizobiales*

[a] Maximum observed log_2 of fold change.
[b] Day of maximum fold change.
[c] All response days.